



Tumor grafted – chick chorioallantoic membrane as an alternative model for biological cancer research and conventional/nanomaterial-based theranostics evaluation

Ana Katrina Mapanao, Pei Pei Che, Patrizia Sarogni, Peter Sminia, Elisa Giovannetti & Valerio Voliani

To cite this article: Ana Katrina Mapanao, Pei Pei Che, Patrizia Sarogni, Peter Sminia, Elisa Giovannetti & Valerio Voliani (2021): Tumor grafted – chick chorioallantoic membrane as an alternative model for biological cancer research and conventional/nanomaterial-based theranostics evaluation, Expert Opinion on Drug Metabolism & Toxicology, DOI: [10.1080/17425255.2021.1879047](https://doi.org/10.1080/17425255.2021.1879047)

To link to this article: <https://doi.org/10.1080/17425255.2021.1879047>



© 2021 The Author(s). Published by Informa UK Limited, trading as Taylor & Francis Group.



Published online: 10 Feb 2021.



[Submit your article to this journal](#)



Article views: 669



[View related articles](#)



[View Crossmark data](#)



Citing articles: 3 [View citing articles](#)

Tumor grafted – chick chorioallantoic membrane as an alternative model for biological cancer research and conventional/nanomaterial-based theranostics evaluation

Ana Katrina Mapanao^{a,b}, Pei Pei Che^{c,d}, Patrizia Sarogni^a, Peter Sminia^c, Elisa Giovannetti^{d,e}
and Valerio Voliani 

^aCenter for Nanotechnology Innovation@NEST, Istituto Italiano Di Tecnologia, Pisa, Italy; ^bNEST-Scuola Normale Superiore, Pisa, Italy; ^cDepartment of Radiation Oncology, Amsterdam UMC, Vrije Universiteit Amsterdam, Cancer Center, Amsterdam, The Netherlands; ^dDepartment of Medical Oncology, Amsterdam UMC, Vrije Universiteit Amsterdam, Cancer Center Amsterdam, The Netherlands; ^eCancer Pharmacology Lab, AIRC Start-Up Unit, Fondazione Pisana per La Scienza, Pisa, Italy

ABSTRACT

Introduction: Advancements in cancer management and treatment are associated with strong pre-clinical research data, in which reliable cancer models are demanded. Indeed, inconsistent preclinical findings and stringent regulations following the 3Rs principle of reduction, refinement, and replacement of conventional animal models currently pose challenges in the development and translation of efficient technologies. The chick embryo chorioallantoic membrane (CAM) is a system for the evaluation of treatment effects on the vasculature, therefore suitable for studies on angiogenesis. Apart from vascular effects, the model is now increasingly employed as a preclinical cancer model following tumor-grafting procedures.

Areas covered: The broad application of CAM tumor model is highlighted along with the methods for analyzing the neoplasm and vascular system. The presented and cited investigations focus on cancer biology and treatment, encompassing both conventional and emerging nanomaterial-based modalities.

Expert opinion: The CAM tumor model finds increased significance given the influences of angiogenesis and the tumor microenvironment in cancer behavior, then providing a qualified miniature system for oncological research. Ultimately, the establishment and increased employment of such a model may resolve some of the limitations present in the standard preclinical tumor models, thereby redefining the preclinical research workflow.

ARTICLE HISTORY

Received 9 December 2020
Accepted 18 January 2021

KEYWORDS

Angiogenesis;
chemotherapy;
chorioallantoic membrane;
nanomedicine; radiotherapy;
tumor models

1. Introduction

Preclinical cancer studies are conventionally performed *in vitro* using monolayers of cell cultures and/or *in vivo* with animal models. Two-dimensional (2D) cell cultures are commonly employed for initial studies due to their relatively easy handling and the availability of numerous standardized methodologies for further analyses. Meanwhile, animal models provide more holistic and systemic conditions that are usually difficult to replicate and maintain *in vitro* [1]. However, the crucial limitations entailed with use of 2D models compel researchers to develop alternative tumor models that reliably mimic the tumor and its microenvironment [2,3]. This demand is further driven by the establishment of more strict regulations toward the use of animals for research purposes, following the 3Rs concept of reduction, refinement, and replacement of animal models [4,5]. As a result, an increasing number of studies on tumor biology and treatment assessments have been utilizing three-dimensional (3D) cell cultures grown as multicellular

tumor spheroids or using scaffolds [6–8]. 3D cell cultures account for the presence of heterogeneous cell population, cell-cell and cell-extracellular matrix (ECM) interactions, and various physiochemical gradients [2,9]. Yet, most of these systems lack the representation of other factors that actively contribute to tumor behavior and treatment response, including the presence of tumor stroma and vascularization [10,11]. Thus, investigations accounting for the effects of the tumor microenvironment (TME) and vascular networks would require a more sophisticated model, such as the tumor-grafted chicken embryo chorioallantoic membrane (CAM) system.

The CAM is a region in fertilized avian or reptilian eggs, which develops after the fusion of the mesodermal layers of the allantois and chorion. In chicken eggs, where hatching happens after 21 days of incubation (Figure 1(a)) [12,13], the CAM begins to form between days 3 to 5 [14]. The CAM is composed of three regions: i) the *ectoderm* from the chorion, which gets attached to the shell, ii) the *mesoderm* in which the blood vessels and stroma are found, and iii) the

CONTACT Elisa Giovannetti  e.giovannetti@amsterdamumc.nl  Department of Medical Oncology, Amsterdam UMC, Vrije Universiteit Amsterdam, Cancer Center Amsterdam, Amsterdam, The Netherlands; Valerio Voliani  valerio.voliani@iit.it  Center for Nanotechnology Innovation@NEST, Istituto Italiano Di Tecnologia, Piazza San Silvestro 12, Pisa, Italy

^{*}These authors contributed equally
Shared senior authors

Article highlights

- Tumor-grafted CAMs are sophisticated biological systems that account for the dynamic roles of the tumor microenvironment and vascular networks in cancer pathophysiology.
- The employment of CAMs in oncological studies conforms to the 3Rs concept of reduction, refinement, and replacement of animal models.
- Aside from being elaborated models for tumor biological studies, tumor-grafted CAMs are also suitable for the continuous streamlining and reliable evaluations of conventional and nanomaterial-based imaging and treatment modalities.
- Although long-term effects cannot be evaluated in these models, crucial data in initial efficacy, potential toxicity, and *in ovo* biodistribution of conventional and nanomaterial-based therapeutics could be obtained upon screening.
- The inclusion of CAM tumor models in the preclinical research workflow may foster the advancement of efficient and safe cancer treatments.

This box summarizes key points contained in the article.

endoderm, which faces the allantoic cavity [15]. The membrane continuously develops and enlarges until it covers the whole yolk sac and gets pressed against the eggshell at 16 days after incubation [14]. The CAM primarily functions as the embryo's respiratory organ, especially during the earlier developmental stages. It also serves as a storage of excretions and facilitates the transport of ions, including sodium, chloride, and calcium [16,17]. In particular, the calcium ions used mainly for bone mineralization are transported from the eggshell to the embryo at a rate of 100 nmol/hour/cm² [16,18]. Blood vessels rapidly form, develop, and rearrange until day 11 of incubation, and the network takes its final form on day 18 [16]. The rich vascular network makes the CAM suitable for studies on vascularization and angiogenesis, including the evaluation of the pro- or anti-angiogenic effects of therapeutics. In this regard, CAM-based biological models also enable investigations on diseases that are significantly affected by angiogenic abnormalities, such as age-related macular degeneration [19], rheumatoid arthritis [20], bone fracture [21], inflammation [22], and cancer [23].

Tumors generally promote the formation of blood vessels in order to assist the transport of nutrients and metabolic wastes, as well as to allow exchanges of gases [24]. Angiogenesis is recognized as one of the hallmarks of cancer and is the target of several therapeutics, including the tyrosine kinase inhibitors (TKIs) bevacizumab, sunitinib, and sorafenib [25]. Thus, the inclusion of tumor tissues on the CAM generates a competent system for investigations on cancer development, angiogenesis, and treatment responses. Other types of tumor models also aim to better represent the dynamics between tumors and vascular network, such as in co-cultures of cancer and endothelial cells [26,27], microfluidics-supported cell culture systems [28–30], or models employing both [31,32]. In most studies, these models are utilized for investigations on tumor-related angiogenesis, metastasis, drug discovery, assessment, and delivery. Nevertheless, their applications may be limited by the absence of blood flow/perfusion, as in the case of cell co-

cultures, and the technical complexity of material microfabrication and biological sample recovery for further analyses in systems employing microfluidics. In contrast, CAM tumor models provide a reliable tumor and TME representation that naturally contain blood vessels, incorporate fluid flow dynamics, and with the tumors accessible for treatment administration and harvesting. Tumor representation can be further enhanced with the addition of relevant cells types, such as human-derived mesenchymal stem cells, which are also involved in certain tumor development processes [33]. Furthermore, CAM tumor models may provide information on off-site tumor behaviors, including metastasis, drug pharmacokinetics, and toxicology [15,18,34].

CAM tumor models offer a number of technical and practical advantages. One of these is the rapid tumor tissue formation, which in various tumor types develops between 2 and 5 days after the cancer cells are deposited. This waiting period is substantially shorter compared to other common animal models like mammalian models, in which tumors need 3 to 6 weeks to grow [18]. Moreover, tumor formation on CAM is favored when the grafting procedure is conducted during the earlier incubation period. It has been noted that toward days 10 to 12 of incubation, immune components like T-cells, B-cells, heterophils, and neutrophils are starting to be present in the developing chick embryo [15,35]. Therefore, grafting at earlier developmental stages takes advantage of the still immature immune responses, allowing various types of tissues to be grafted with lower rejection rate. CAM tumor models are also easily handled during some imaging and treatment evaluations, as anesthetization and procedures for movement restrictions of the host can be conveniently performed or completely excluded [36,37]. Furthermore, different administration routes can be evaluated, including intravenous, topical, and intraperitoneal, with the tumor development and treatment outcomes accessibly observable in real-time [18]. These models are also amenable to medium/high-throughput analyses, are cost-effective in comparison to other small animal models, and do not require a specialized and sterilized laboratory. Finally, CAM tumor models do not require a permission or an approval from animal research ethics committees, depending on a country's legislation [18]. As territorial regulations on the use of animals for scientific research purposes may vary, in most countries, however, less strict rules apply on CAM experimentations, provided that studies are terminated prior to hatching or development of pain perception [16,18]. These conditions have been stressed in the statement of the National Institute of Health and the Institutional Animal Care and Use Committees (United States of America) that the label 'live vertebrate' applies to avian models post-hatching [38]. Instead, legislation in other nations includes the latter half of avian embryo development under the protection of animals [39]. Member states of the European Union uphold directive 2010/63/EU to offer protection to mammals, but also applies to fetal forms of mammals in their last third of embryo development. However, these rules do not state that they also extend to fetal avian embryos [40]. Most importantly, these

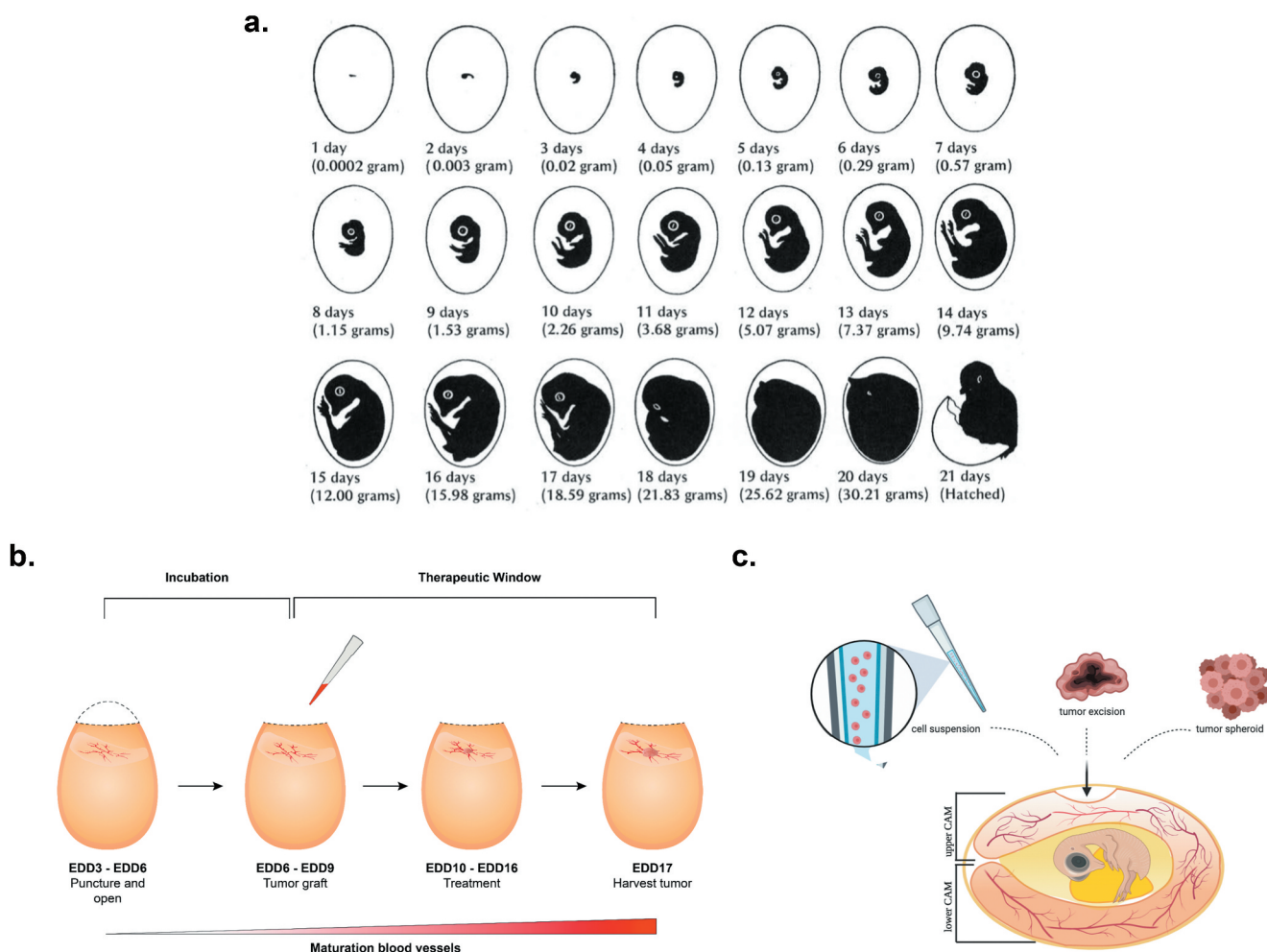


Figure 1. (A) Embryonic development and accompanying changes in the weight of the chick embryo (white leghorn). The given weights are from the chick embryo corresponding to each embryonic developmental day. These weights could be useful for initial dose-screening of the drug in order to determine the maximal tolerable dose with regards to embryo viability by computing interspecies allometric scaling for dose conversion. Alternatively, dose-escalation studies could be performed prior to further (combination) studies. Adapted from Romanoff (Cornell Rural School Leaflet) [12] and Smith [13], Copyright 2019 by the Mississippi State University Extension Service. (B) Schematic overview of the CAM as an *in vivo* tumor model. Fertilized chicken eggs are punctured on EDD3 and the resulting hole will be enlarged on EDD6. Then, tumor cells will be grafted and incubated for 4 days. Typically, the therapeutic window spans over 10–12 days, after which the tumor is harvested and processed for downstream applications. Adapted from Kleibeuker et al., 2015 [37]. (C) Tumors are commonly grafted onto the CAM by depositing a cell suspension, tumor excision, or pre-made 3D cell constructs such as spheroids. Adapted from Kim et al., 1998 [57].

ethical guidelines are commonly established for humane treatment and euthanasia of the animal models.

Albeit the significant advantages, tumor-grafted CAMs also demonstrate a number of limitations. For instance, despite the fast formation of some tumors, the time to perform experimentations is strictly limited to weeks. This duration may be inadequate to observe processes like the evident growth of tumors in secondary sites [14]. Also, while acute treatment effects could be evaluated, the follow-up time for evaluation of delayed effects is too short. Moreover, later incubation periods may involve nonspecific inflammatory responses as the immune system of the embryo begins to develop [16]. The physiological development inside the fertilized egg happens rapidly and even a single day can impose variabilities in conditions that can consequently affect the tumor development [18,41]. These further stress the need to develop standardized protocols, in which the tumor grafting procedures are performed at earlier

incubation stages, consistently on the same period, and under the same conditions (Figure 1(b)). Another concern would be the tendency of tumor grafting to trigger vascularization, which may be difficult to distinguish from the innate angiogenesis of the developing embryo in absence of the tumor [14]. The system is also sensitive to changes in external conditions like temperature and humidity. Post-CAM assay experiments, such as histological and biomolecular studies, are also constrained by the limited number of commercially available reagents that are compatible with avian samples [34]. Using the reported chick genome can be taken advantage of to design reagents to distinguish the chick and human samples [42,43].

Nevertheless, the CAM tumor model remains to be one of the most accessible and reliable systems with an elaborated representation of the disease and is applicable for various oncological investigations [14,15]. Its availability allows streamlining of conventional treatments, making rapid

evaluations following alterations, such as after changing drug or radiation dosages, scheduling of administration, and sequences of treatments [44,45]. Likewise, it gains additional importance in evaluating emerging technologies for cancer applications, most notably in the assessment of nanomaterial-based platforms for disease imaging and treatment. Thus, the CAM tumor model is gradually finding relevance within the preclinical cancer research workflow, especially for a stronger demonstration of proof of concept of technologies and approaches for cancer treatment [18].

In this review, the increasing applicability of CAM tumor models is demonstrated, specifically highlighting pertinent studies on tumor biology and evaluation of conventional and nanomaterial-based technologies for cancer imaging, diagnosis, and therapy. The common techniques and assays performed to evaluate the CAM tumor systems are described, while additional insights and future perspectives are elaborated. This review aims to exhibit the relevance of CAM tumor models and to further encourage their application in preclinical research. The CAM tumor models have great potentials in the development and translation of efficient and safer cancer treatments to the clinical practice.

2. Tumor-grafted chorioallantoic membrane as an adaptable oncological model

Studies utilizing CAM tumor models can be dated as early as 1911 [46], and since then, several methods and techniques to construct these oncological systems have been reported [34]. Generally, the membrane is deposited with cells either in suspension or premade into 3D constructs, or with an excision of tumor tissue (Figure 1c) [37,47,48]. Complementary procedures have been further integrated to optimize tumor growth, for instance by varying the number of the inoculated cells, using supporting materials like Matrigel® and silicone or Teflon rings, and lacerating the membrane to damage the outer chorion layer to deliver the cells on the mesoderm and promote vascularization [37,49,50].

The following section highlights the successful application of the CAM in angiogenesis and metastasis studies, as well as for investigations on biomolecular pathways and potential targeting discovery. Subsequently, the adaptable employment of these models in a wide range of tumor imaging and treatment studies is elaborated, through discussion of a number of investigations on conventional and nanomaterial-based oncological platforms.

2.1. Examining cancer biology using CAM tumor models

Chromosomal instability is another hallmark of cancer caused by chromosome segregation error during mitosis, and leads to small insertions or deletions and numerical chromosomal abnormalities [51,52]. Although these instabilities generate copy number variation in cancer cells, the aggressiveness and invasive properties of the tumor depend on the type of the nucleotide change and the surrounding sequences, which may physically or chemically affect mutagenesis [53].

Moreover, tumor-promoting genetic alterations enable cancer cells to cross the basement membrane, invade the connective tissue and the surrounding stroma, actively enter in the vasculature (intravasation), survive in the circulation, and reach distal sites from the primary tumor (metastasis) [54,55]. These oncological processes serve as rate-limiting steps for the metastatic cascade and involve mechanical interaction between the cancer cells and their microenvironments [56]. Indeed, several factors may potentially influence the ability of the cancer cells to intravasate into the circulation, including defects in adhesion to endothelium and the rate of *in vivo* proliferation [57]. These behaviors may vary among different cancer cell lines, along with their capacity to escape from the primary tumor [24].

The chick embryo CAM represents a useful system for the investigation of tumor cell invasion and metastasis, and offers to overcome many experimental limitations found in other *in vivo* systems [58]. The CAM tumor model allows identification and detection of the key molecules that are pathologically involved in tumor-promoting processes [57]. Furthermore, the microcirculation and differential extravasation behaviors of several cancer types can be conveniently observed and quantified [59].

2.1.1. The role of angiogenesis in tumor development

Angiogenesis, which is the formation of new blood vessels from preexisting vasculature, is vital during embryonic development and regulates several biological processes during adulthood [60,61]. The generation of new vasculature is crucial in various physiological processes like wound healing and tissue regeneration, but is also highly activated in pathogenesis as in tumor invasion and progression (Figure 2(a)) [62]. The CAM can be suitably used for angiogenesis-related cancer studies due to its high vascularization, which sustains the engrafted tumor with nutrients and provides a conducive environment for tumor growth. Various cancer cell types have demonstrated such behavior, in which grafting onto the CAM causes the formation of solid tumors with rich vascular networks (Figure 2(b)), and also allowed the cells to migrate from the primary tumor site [34,63]. Grafted tumor specimens go through an avascular phase of about 72 h before blood vessels begin to infiltrate the tumor. Then, tumor volume and mass rapidly increase during the vascular phase. These dynamics have been deduced after observing the disappearance of the necrotic core from the tumor in avascular phase, which eventually reappears when the newly formed blood vessels could no longer sufficiently support the matured tumor [64]. Nonetheless, compared to normal blood vessels, the tumor blood vessel architecture is aberrant, with dilated vessels, distributed chaotically and unevenly, and with irregular branching patterns (Figure 2(a)) [65].

Several ligand-receptor signaling pathways are associated with angiogenesis and cancer progression, whereas vascular permeability may allow tumor cells to intravasate and circulate, hence metastasize [66]. The invasive behavior of cancer cells is concomitant with the overexpression of the

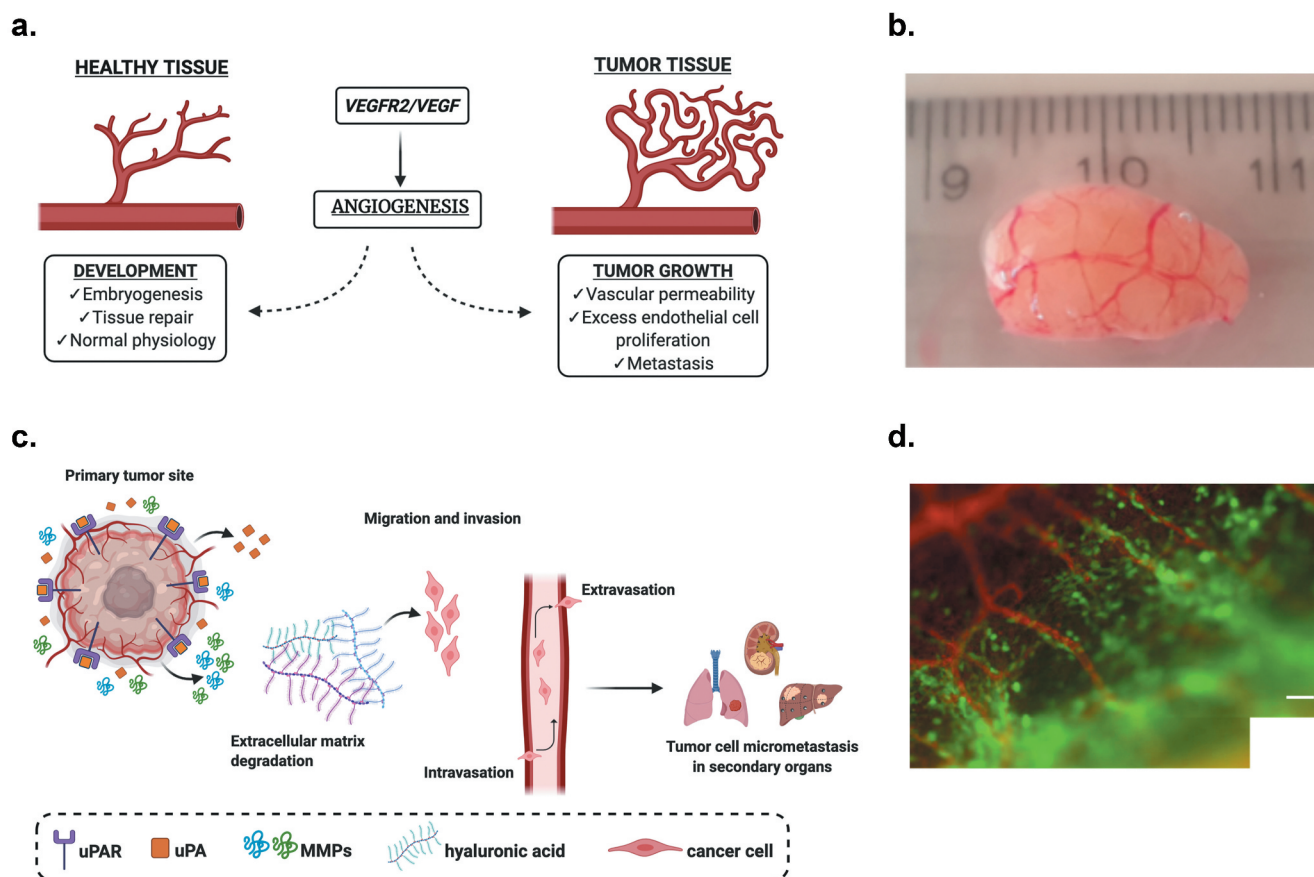


Figure 2. (a) Angiogenesis is regulated by VEGFR/VEGF in both healthy and tumor tissue. But unlike normal blood vessels, tumor vascular networks are chaotic and show an irregular architecture that permits tumor metastasis. (b) Suit2.28 wild-type pancreatic tumor harvested 11 days after grafting, surrounded by rich vascularization (unpublished data). (c) Overview of invasion and metastasis processes. An elevated expression of uPA/uPAR in concomitant with MMPs activity allow the degradation of the ECM and the migration of tumor cells from the primary tumor site by generating micrometastasis foci in distal regions. (d) High disseminating fibrosarcoma cells (HT-hi/diss) demonstrate vasculotropic behavior, in which the cells (green) move away from the primary tumor site and toward the nearby blood vessels (red); scale bar = 50 μ m. Reproduced with permission from Deryugina and Kiosses [81]. Copyright 2017 by the authors.

epidermal growth factor receptor (EGFR) and vascular endothelial growth factor (VEGF), and the production of matrix metalloproteinases (MMPs) [66]. Tumor-induced angiogenesis may correspondingly reflect the aggressiveness of tumor and has become a reliable prognostic indicator for cancer progression [67]. Additionally, characterizing the blood vessel phenotype may provide more comprehensive insights into the vascular origin. For this purpose, anti-CD31 antibody, *Simbacus nigra* 1 isolectin, and anti-desmin have been used to respectively detect human-derived blood vessel, chick blood vessel, and vessels from both species [68]. The high expression levels of VEGF and VEGF receptor-2 (VEGFR-2) in the CAM were found to be vital for the vascularization, with the peak of detection at the 11th embryonic day of development (EDD) of the incubation period [69,70]. Upregulation of VEGFR-2 expression was also found in immature neovessels during glioma development [71]. Similarly, human head and neck squamous cell carcinoma and colon carcinoma were found to stimulate neovascularization and induce high angiogenic responses from the host following CAM grafting procedures [72,73]. Accordingly, anti-VEGF treatment of colon carcinoma cells was shown to significantly reduce tumor-induced angiogenesis,

consequently restoring the angiogenic index to the level of non-metastatic colon carcinoma cell-variant [73].

Angiogenesis studies using CAM tumor models can be further extended to patient-derived xenografts (PDX). Grafting of freshly harvested tumor specimens onto the CAM advantageously preserves various components of the original TME associated with the *in vivo* angiogenic response [74]. Therefore, CAM-PDX models are finding increased relevance in precision medicine [48]. Differences in tumorigenic and angiogenic behaviors between cell lines and patient-derived tumor samples have been documented. For instance, Klagsbrun *et al.* [75] used human glioblastoma and meningioma cell lines and patient-derived glioblastoma and meningioma specimens to study their vascular responses upon grafting onto the CAM. Blood vessel density from patient-derived brain tumor cells was significantly increased compared with glioma cell lines. This relatively high angiogenic potential was accompanied by an increased production of a mitogenic factor for vascular endothelial cells [75]. The Tumor Angiogenesis Factor (TAF) stimulates the endothelial cells to produce two proteolytic enzymes: the plasminogen activator (PA) and collagenase, which are both necessary to invade and degrade tissues near the endothelial cells [76].

These findings are consistent with the fact that brain tumors are one of the most highly vascularized types of cancer [77]. The CAM tumor model can also be used to evaluate the angiogenic potentials induced by normal and malignant lymphocytes. Tissue biopsy derived from Hodgkin's disease, with malignant lymphocytes, showed positive vascular response resulting in increased vascularization on the CAM [78].

2.1.2. Tumor invasion and metastasis

The detection of several biomolecules allows semi-quantitative analyses of tumor metastasis within the chick embryo system. For example, urokinase plasminogen activator (uPA) is a serine protease involved in ECM degradation, cell migration, and metastasis. An elevated expression of uPA has been observed in various types of cancer, and a link between cancer cell uPA, its receptor plasminogen (uPAR), and metalloproteinase was proposed and associated with invasion and metastasis (Figure 2(c)) [79]. Kim and colleagues [57] utilized uPAR to examine the intravasation properties of HEP3 oral squamous cell carcinoma grafted on CAM. Four clones of HEP3 cells transfected with a vector expressing anti-sense RNA against uPAR were compared to the parental Hep3 cells transfected with vector alone. Reduction of up to 70% of uPAR completely blocked the intravasation capacity of cells [57]. Nevertheless, even though the presence of human uPA in the organ of the embryo serving as a secondary tumor site can be used as a quantitative marker for metastasis, it is limited to metastasized cells with moderate to high expression levels of uPA [80].

The CAM tumor models have also been vital in monitoring metastasis in certain cancer types. For instance, the different metastatic behaviors of HEP3 and HT1080 fibrosarcoma tumors have been identified through quantification of the human-specific *Alu* sequence in the lungs of the embryo, which served as the secondary tumor site. The results confirmed the high metastatic potential of epidermoid carcinoma, as HEP3 cells efficiently disseminated from the primary tumor site and grow in the lungs. On the other hand, the inferior metastatic profile of HT-1080 cells was associated with their lower rate of intravasation and the delayed growth and expansion at the secondary tumor site [58].

Other notable and targeted cancer-promoting biomolecules are the MMPs, which are matrix-degrading enzymes that support metastasis [24]. The role of MMPs in the intravasation process has also been investigated using human HT-1080 fibrosarcoma-grafted CAMs. Additionally, two isogenic variants with 50 to 100-fold difference in disseminating behavior (high disseminating: HT-hi/diss and low disseminating: HT-lo/diss) were established using CAM systems. Both variants were able to develop primary tumor sites on the CAM. Yet, regardless of the tumor growth and size, HT-lo/diss appeared to be more restrained within the vicinity of the primary tumor while HT-hi/diss invaded the adjacent blood vessel and mesoderm. Fluorescently labeled HT1080 cells further illustrated the invasive and

vasculotropic properties of HT-hi/diss, in which 25% of the migrating cells in the stroma were found to be in close contact with the nearby blood vessels, compared to less than 3% in the HT-lo/diss variant (Figure 2(d)) [81]. These behaviors were significantly different from the observations on 2D cell cultures, in which both variants showed similar proliferation, migration, and adhesion properties. The invasive behavior of HT-hi/diss was associated with the action of biomolecules like MMPs, which affect the cell-cell and cell-matrix interactions and promote migratory responses. While the efficient downregulation of MMP-14 did not affect tumor dissemination, an unexpected threefold increase in intravasation and metastasis was documented following the substantial downregulation of MMP-9 using specific small interfering RNA (siRNA) and function-blocking monoclonal antibody (mAb) [82].

The abovementioned study of Deryugina *et al.* further demonstrates that the highly vascularized lower CAM may serve as a repository of intravasating tumor cells. While the upper CAM refers to the upper half of the egg on which the tumor is grafted, the lower CAM denotes the other half that is away from the grafting site and is connected to the tumor only by blood and lymphatic vessels [57,82] (Figure 1(c)). Therefore, the ability of cancer cells to colonize that CAM region may also provide insights into their metastatic behavior. Conventional mammalian models lack such particular compartments, which may also be easily dissected out for further analysis [82]. In this regard, Subauste and coworkers [73] harvested sections of CAM inoculated with aggressive human colon cancer cells pre-labeled with green fluorescent dye. The vasculatures were also fluorescently labeled for distinctive imaging with the cancer cells. The results showed that SW480 and SW620 colon cancer cell lines behave differently when inoculated on CAM, *i.e.* while majority of SW480 cells disappeared from the CAM and were detected in the ectoderm capillary plexus, SW620 cells proliferated and developed large metastatic foci that extended into the mesodermal layer of the CAM [73]. The same group evaluated the implications of CDCP1 on tumor foci formation and metastasis on CAMs grafted with fluorescently labeled HeLa cells overexpressing CDCP1. A significant reduction in vascular colonization was observed on tumors treated with the CDCP-1 inhibitor mAb 41-2. The authors further suggested that mAb 41-2 limits the number of micrometastasis foci instead of reducing the number of cells in each focus. The antitumor effects were also corroborated with *in vitro* studies, in which the inhibitor caused enhancement in tumor cell apoptosis [15].

Overall, it is tempting to claim that most of the earlier applications of CAM tumor models focused principally on understanding cancer biology and identifying vital biomolecules that drive angiogenesis and tumorigenesis. Several of the recent studies are instead utilizing these models for pharmacological and toxicological evaluations of antitumor

therapeutic candidates. Nevertheless, findings on tumor biology and dynamics are still needed and will remain vital, especially to identify and conceptualize novel strategies for improved cancer management and treatment.

2.2. Assessment of conventional treatment modalities in preclinical cancer research

In cancer treatment, surgery, radiotherapy, and chemotherapy remain as the three core modalities to treat patients for a variety of tumor types. With precision medicine in mind, the use of animal models to effectively assess treatment strategies *in vivo* could considerably contribute to select subgroups of patients that are likely to respond to the treatment. By using PDXs for example, the heterogeneity and pathophysiological features of the patient could be recapitulated into these models, allowing detailed analysis of the molecular and cellular responses to treatment.

Over the years, patient-derived cancer cells and established cell lines from different types of solid tumors have been successfully grafted on the CAM including breast [83–86], colorectal [44,87], pancreatic [11,88], prostate [89], brain cancer [90,91], and many more [92–94]. Like rodent models, the CAM model could be used to assess the effects of conventional modalities used in the clinic to treat cancer, including chemotherapeutics, radiation-based or targeted therapy. Its versatility as a preclinical model is further highlighted as a potential tool to assess microsurgical techniques [95]. Patient-derived tumor cells grown on the CAM were also shown to maintain genetic mutations similarly found in the original pancreatic ductal adenocarcinoma (PDAC) tumors [11], and reproduce certain pathophysiological hallmarks of the disease like in human glioblastoma [90]. Genetically engineered tumor cells could also be utilized, increasing the options to measure tumor growth noninvasively [11,96]. These, along with many other studies, had led to open up the CAM as a potential platform to optimize conventional treatment schedules, assess experimental therapeutic strategies, or even tumor progression with the perspective for personalized treatment [11,44,48,91].

While technical advances have been made over the decades to improve therapeutic outcomes, localized failure or resistance to systemic treatment has led to increasing interest in combination treatment such as chemoradiation or the addition of a targeted drug. In the following section, we discuss the most recent data for each conventional cancer treatment modality and highlight the suitability of the CAM for evaluation of novel combination treatments and mechanistic laboratory studies.

2.2.1. Applications in imaging and detection

A crucial part of cancer treatment is the detection and imaging of tumors. For instance, the delineation of the tumor against normal healthy tissue plays an integral part in radiotherapy in order to precisely deliver radiation doses only to the tumor site and spare the neighboring healthy tissues. Furthermore, tumor response during the course of a treatment could be monitored

in patients. By combining imaging techniques like positron emission tomography (PET) with magnetic resonance imaging (MRI) or computerized tomography (CT) a variety of functional and morphological information could be acquired. Notably, the use of radiolabeled compounds and contrast agents for PET and MRI, respectively, have led to the need for suitable models for biodistribution and target specificity studies (Figure 3). The emergence of the CAM and its utility for imaging studies have been extensively reviewed [97]. The CAM offers, in a relatively quick and cost-effective manner, a platform to perform initial evaluations of novel MRI contrast agents and radiolabeled PET tracers. The latter was studied by Warnock *et al.* [98] in tumor-bearing chick embryos where the biodistribution of injected ^{18}F -FDG, ^{18}F -Na, or ^{18}F -TYR could be followed in a small animal PET system. Notably, combining CT and PET scans allowed accurate imaging and better distinction of the human glioblastoma tumor, as a high uptake could similarly be observed in the chick embryo (Figure 3(a)) [98]. Moreover, the addition of CT or MRI scans to PET could provide relatively accurate tumor volume estimation, as *in ovo/vivo* CT and *ex ovo/vivo* CT scans of the tumor were found to be comparable. In a similar manner, this was also the case for PET/MRI scans, where target-specificity was evaluated *in ovo* for prostate-specific membrane antigen (PSMA) positive and negative prostate carcinoma xenografts (Figure 3(b)) [99]. Previous mouse xenograft studies using the same PSMA-specific tracer demonstrated comparable accumulation values for both mice and CAM models. To obtain high-resolution images, motion artifacts due to sudden movements of the chick embryo should be prevented. Anesthetics have been delivered to the chick embryo through fumigation or topical administration [98–100]. Alternatively, eggs could be pre-cooled at 4°C for at least 1 hour prior to imaging [83].

2.2.2. Pharmacological studies using CAM-grafted tumors

As the CAM provides a highly vascularized bed to study angiogenesis in oncology, many studies have focused on targeting this process with small molecules [24]. Lin *et al.* [101] showed via *in vitro* and *in ovo* assays that anlotinib better exhibited anti-angiogenic properties in comparison to other TKIs sunitinib, sorafenib, and nintedanib. Similarly, this allowed for characterization of lead compound TKI-31 for potential anti-angiogenic properties [102]. Sunitinib, for example, has been widely used in a variety of cancers, but patients gradually develop resistance against the drug [103–105]. D'Costa *et al.* [106] demonstrated, using sunitinib-resistant and wild-type renal cell carcinoma cell lines, that combining sunitinib and ATP-binding cassette subfamily B member-1 (ABCB-1) inhibitor elacridar could reduce tumor growth on both the CAM and in murine models. Kleibecker *et al.* [44] assessed the potential of sunitinib in combination with ionizing radiation (IR) in colorectal cancer. First, they showed that tumor growth inhibition was schedule-dependent. Next, tumor growth delay was observed only when tumor grafts were treated with sunitinib prior to radiation. Their data demonstrated that

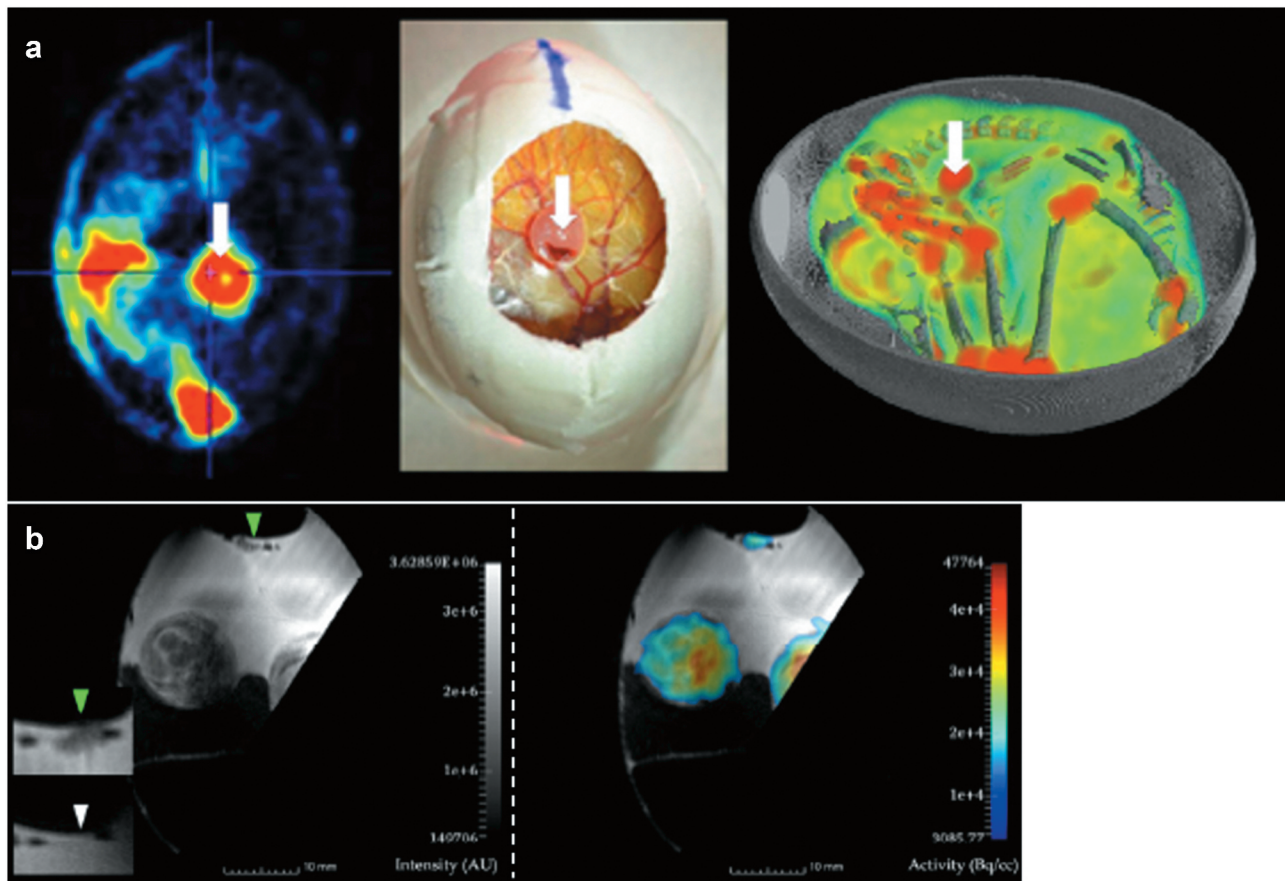


Figure 3. Conventional tumor imaging modalities have been applied on CAM tumor analyses. (a) Examples of human glioblastoma U87 (white arrows) and the chick embryo visualized via co-registered PET/CT (left), photograph (middle) and 3D overlay of PET and CT images post-administration of ^{18}F -FDG. Reproduced from Warnock et al. [98]. Copyright 2013 by the Society of Nuclear Medicine and Molecular Imaging, Inc. (b) MRI (T2-weighted, left panel) and PET/MR fusion images (right) of PSMA-positive LNCaP C4-2 prostate carcinoma. Green and white arrows indicate PSMA (+) cells and CAM, respectively. Reproduced from Winter et al. [99]. Copyright 2020 by the authors.

optimization of dose-scheduling allows halving of the dosage of sunitinib without loss of therapeutic efficacy. On a different note, Rovithi *et al.* [11] were able to treat patient-derived PDAC with gemcitabine and crizotinib in CAM xenografts. They showed that this combination could effectively reduce tumor growth as compared to monotherapy. To elucidate potential mechanisms of actions, they subsequently studied microRNA expression profiles derived from CAM xenografts [11].

As the CAM provides an accessible platform enabling researchers to study tumors formed in a vascularized environment, other experimental interventions could be more readily evaluated, such as mast cell stabilizer disodium cromoglycate – more commonly associated with asthma relief – or anti-podoplanin antibodies against fibrosarcoma-like tumors [107] or use of endostatin in renal cell carcinoma [108]. Drug delivery systems containing drugs, either encapsulated with polymers or liposomes, could also be assessed in this small animal model for their distribution within the chick embryo and will be discussed in greater detail in section 2.3.

2.2.3. Radiation-based studies using the CAM model

Within the field of radiation oncology, side-effects of radiotherapy are often associated with injury to the surrounding vasculature [109,110]. Another obstacle is the intrinsic radioresistance, urging further exploration of combining IR with other cancer treatment modalities [111,112]. The combination of IR with different – radiosensitizing – treatment modalities, has been a focus of several studies using the CAM as a surrogate *in vivo* model [94,113]. Kähler *et al.* [114], for example, used the CAM to study the mechanism behind radioresistance in head and neck squamous cell carcinoma. Radiosensitization studies with the intravenously administered hypoxic cell sensitizer etanidazole prior to a single radiation dose of 8 Gy showed decreased tumor weight, suggesting a radiosensitizing effect in the CAM [115].

Adverse effects of radiation to normal tissues are mostly the result of damage to the existing, mature, vasculature, which are typical late effects of radiation, and manifest in months to years after exposure [116]. The limited time frame of the CAM model only allows the evaluation of early vascular responses. This is a different, yet highly interesting issue, since effects of radiation could be studied on proliferative and maturing blood vessels. Kleibeuker *et al.* [44] observed that a single dose of 4 Gy was the maximum tolerable radiation

dose in white leghorn chick embryos on EDD6. Based on vascular parameters such as vessel length, number of ends and branch points of the blood vessels, a reduction of respectively 50% and 10% was observed in irradiated CAM on EDD6 and EDD12. Similar results were observed when chick embryos were irradiated with 10 Gy at EDD9 and EDD13 with a reduction in total blood vessel length and area of approximately 20–40% and 5%, respectively [117]. Even vascular injury at high entrance doses of 200 to 300 Gy via microbeam radiation is dependent on the maturation of the CAM vasculature [118]. Taken together, immature and growing blood vessels are more prone to IR as opposed to mature blood vessels. This is in line with the radiobiological principle that fast-proliferating cells are highly sensitive to radiation. Interestingly, recovery was observed within three days after IR-induced reduction of these vascular parameters, indicating that these effects are transient [44]. Hence, most studies are performed between EDD6 and EDD10, where the angiogenesis process takes place at its highest rate. While most conventional treatments use relatively high-dose IR, low-dose IR studies on adipocyte angiogenesis could also be conducted on the CAM [119]. It has been shown that conditioned medium from adipocytes exposed to 0.3 Gy could increase the number of blood vessels, indicating a trigger of angiogenesis. Interestingly, combination treatments have also been conducted using radiosensitizers to study potential increase of anti-angiogenic effect. In combination with either single or fractionated irradiation, paclitaxel was not shown to provoke radiosensitization using the CAM angiogenesis model on EDD9 [120]. Unfortunately, the researchers did not further explore potential radiosensitivity with pre-treatment of paclitaxel, as scheduling was indeed shown to be crucial.

Apart from evaluation of the graft rate of previously irradiated tumor cells and assessment of tumor growth following radiation exposure, the CAM model could also be applied to study the so-called tumor bed effect (TBE). The TBE points to the slower rate of tumor regrowth after irradiation due to radiation injury to the vascular-connective tissue and reduced angiogenesis in the 'vascular bed', which is eminently influencing both grafting and the kinetics of tumor growth. Such experiments reflect the clinical situation of recurrent tumors. Tumor cells generally recur in the original, previously irradiated, volume [121]. To our knowledge, no TBE studies have been performed by grafting tumor cells or tumor tissue specimens on the pre-irradiated CAM. Monitoring of the TBE on the molecular and cellular levels would be of particular interest in the early phase of maturing blood vessels starting around EDD5.

2.3. Assessment of novel nanomaterial-based systems for oncological applications

The increasing number of novel platforms aiming to improve cancer diagnosis and therapy intensifies the demand for qualified preclinical tumor models. Nanomaterial (NM)-based imaging and treatment systems are among the leading innovative technologies, which gained further considerations following

the approval for clinical use of Caelyx® (doxorubicin liposomal formulation; also known as Doxil® in the US), Abraxane® (albumin-bound paclitaxel approved for breast cancer, non-small cell lung cancer, and pancreatic cancer), Onivyde® (liposomal formulation of irinotecan for pancreatic cancer), and other nanoformulations of known approved anticancer agents [122]. Nowadays, nanoparticles (NPs) are mainly developed to facilitate drug/cargo delivery and mitigate off-site adverse effects [123]. Cellular experiments using both the conventional 2D and more sophisticated 3D tumor models are mainly employed for preliminary NP assessments [9]. Nevertheless, these models lack the influences of the tumor stroma, ECM, and vascular networks, which likewise contribute to the development and treatment response of the tumor. Hence, tumor-grafted CAMs provide useful advanced biological systems for the continuous streamlining and reliable evaluation of NMs (Table 1).

2.3.1. NM optimization

One of the most interesting features of NMs is associated with their design and functional versatility. However, optimizations in NMs synthesis and properties are necessary in order to maximize their efficiency. The action and *in vivo* behaviors of NMs are strongly dependent on their physicochemical properties like size, shape, and surface features [124]. Among the inorganic NPs proposed for various clinical purposes, silica NPs offer stable materials for cargo delivery with the possibility of conjugation of surface moieties for targeted delivery [123]. To identify the optimal size for delivery of doxorubicin, Bouchoucha and coworkers [125] synthesized mesoporous silica NPs with varied sizes while retaining other physicochemical properties. Melanoma- and fibrosarcoma-grafted CAMs were employed to investigate the NP accumulation, penetration, and release of encapsulated doxorubicin. Better antitumor action was observed on drug-loaded NPs with average diameter of about 45 nm compared to NPs with diameter of 150 nm. The effects were attributed to the deeper tumor penetration of smaller NPs and enhanced chemotherapeutic action due to drug encapsulation, resulting in tumor shrinkage and decrease in weight [125].

Viral nanoparticles are another promising class of NMs for cargo delivery, which take advantage of the innate efficiency of viruses to infect host cells [126]. In this regard, it was demonstrated that the shapes of viral NPs affect in tumor accumulation. Filamentous and spherical viral NPs were both able to accumulate in CAM fibrosarcoma and squamous cell carcinoma models, but an increased tumor penetration was observed with the filamentous NPs. Aside from the shape, the surface charge also affected the intratumoral NP diffusion. Indeed, the positive zeta potential of filamentous viral NPs prevented attractive interactions with the positively charged collagen in the ECM [127]. Alternatively, modifications on the virus capsid can promote tumor accumulation as demonstrated by the coating of the surface of spherical cowpea mosaic virus NPs with polyethylene glycol (PEG) [128]. Surface coating with PEG (PEGylation) is commonly employed

Table 1. Nanomaterial studies performed on tumor-grafted CAMs.

Cell Line	Grafting Conditions	Nanomaterial Description	Reference
<i>Nanoparticle Optimization</i>			
HT1080 fibrosarcoma and M21 melanoma	3.5 x10 ⁵ cells/egg for HT1080 and 1.5 x 10 ⁶ cells/egg for M21	Mesoporous silica NPs loaded with doxorubicin	[125]
HT1080 fibrosarcoma and HEP3 epithelial carcinoma	~1 x10 ⁵ of GFP-expressing cells injected onto the CAM on day 9, <i>ex ovo</i>	Plant viral NPs derived from <i>Potato virus X</i> (filamentous) and <i>Cowpea mosaic virus</i> (spherical)	[127]
HT-29 colon cancer	10 ⁴ to 10 ⁵ cells microinjected on day 9, <i>ex ovo</i>	<i>Cowpea mosaic virus</i> -derived NPs loaded with fluorophore and/or with PEGylated surface	[128]
PC-3 prostate cancer	5 x10 ⁵ cells in medium/Matrigel (1:1 v/v) grafted on day 6, into a silicone ring placed onto the CAM	Polystyrene NPs functionalized with carboxyl (-COOH) and amino (NH ₂) groups	[131]
THP-1 monocytic leukemia	2 x 10 ⁶ cells in medium/Matrigel (1:1 v/v) grafted on day 8	Polystyrene NPs functionalized with carboxyl (-COOH) and amino (NH ₂) groups	[132]
MDA-MB231 breast cancer and PC-3 prostate cancer	7 x10 ⁵ for PC-3 and 1 x 10 ⁶ for MDA-MB231 in medium/fetal calf serum (1:1 v/v) or medium/Matrigel (1:1 v/v; native or growth factor-reduced Matrigel); grafting on day 8	Mesoporous silica NPs functionalized with folic acid or polyethyleneimine, and loaded with γ -secretase inhibitor	[50]
PC-3 prostate cancer	5 x10 ⁴ GFP-expressing cells microinjected on day 10	<i>Cowpea mosaic virus</i> NP functionalized with pan-bombesin analogue, targeting gastrin-releasing peptide receptors	[137]
ML-1 thyroid cancer	1 x10 ⁶ cells in PBS/growth factor-reduced Matrigel (1:1 v/v) grafted on day 8, into a silicone ring placed on the CAM	Mesoporous silica NPs conjugated with methotrexate and loaded with fingolimod	[138]
<i>Nanomaterial-facilitated tumor imaging</i>			
MDA-MB231 breast cancer	2 x10 ⁶ cells suspended in 50% Matrigel grafted on day 7, into a silicone ring placed onto the CAM	Protein-based polypeptide copolymer NPs containing Gd-DOTA (cHSA-PEO(2000) ₁₆ -Gd)	[140]
GL-261 glioma	2.5 x10 ⁵ cells in DMEM, incubated with NPs 8 h prior to grafting on day 10	Ultrasmall gadolinium oxide (Gd ₂ O ₃) NPs	[141]
LS174T and SW480 colorectal adenocarcinoma	5 x10 ⁶ cells in Matrigel grafted on day 8	Cyanine derivative encapsulated in iron oxide NPs with surface functionalized with peanut agglutinin and anticarcinoembryonic antigen antibodies (αCEA)	[142]
NuTu-19 ovarian cancer	10 ⁶ cells in medium/Matrigel (1:1 v/v) grafted on day 8, into a silicone ring on the CAM	Hypericin-loaded polylactic acid NPs	[144]
MCF-7 breast cancer	Premade multicellular tumor spheroids (~500 μm in diameter) grafted on day 9 or 10, <i>ex ovo</i>	Yb- and Er-containing upconversion NPs functionalized with estrogen receptor-α monoclonal antibody	[47]
<i>Nanomaterial toxicity</i>			
U87 glioblastoma	3–4 x10 ⁶ cells in culture medium grafted on day 6, in silicone ring placed on the CAM	Ultradispersed detonation diamond and microwave-radiofrequency carbon allotrope NPs	[147]
U87 glioblastoma	5 x10 ⁶ cells in culture medium grafted on day 6, in silicone ring placed on the CAM	Silver NPs	[148]
U87 glioblastoma	3–4 x10 ⁶ cells in culture medium grafted on day 6, in silicone ring placed on the CAM	Platinum NPs	[149]
BEAS-2B human bronchial epithelial cells and A549 lung adenocarcinoma	3 x10 ⁶ cells in serum-free medium/Matrigel (1:1 v/v) grafted on day 9	Tungsten carbide cobalt (WC-Co) NPs	[150]
<i>Nanomaterial-facilitated tumor treatment</i>			
A.) OVCAR-8 ovarian cancer B.) Ovarian cancer patient sample	A.) 2 x 10 ⁶ GFP-expressing cells grafted on day 10 into a Teflon ring placed onto the CAM B.) Samples were minced into pieces of approximately 1 mm, and placed on top of CAM	Doxorubicin-loaded mesoporous silica NPs	[156]
786-O renal carcinoma	1 x10 ⁶ cells in medium/Matrigel (1:1 v/v) grafted on day 7	Poly(lactic-co-glycolic acid) conjugated with tetraiodothyroacetic acid (Tetrac),	[157]
HT1080 fibrosarcoma	~2.2 x10 ⁴ cells (alone or with NPs) in collagen/medium mixtures grafted on day 8	Gold nanorods coated with mesoporous silica, loaded with doxycycline, fosbretabulin, and indocyanine green; surface functionalized with RGD peptide	[158]
MDA-MB231 breast cancer	5 x10 ⁵ firefly luciferase-expressing cells in medium/Matrigel (1:1 v/v) grafted on day 7 into a silicone ring placed onto the CAM	Human serum albumin-based polyethylene glycol NPs containing doxorubicin and Gd DOTA (dcHSA-Gd-Dox)	[160]
EMT6 murine mammary carcinoma	7 x10 ⁶ cells in medium grafted on day 9 into a Teflon ring placed on the CAM	Liposomal formulations of meta-tetra(hydroxyphenyl) chlorin (mTHPC): Foslip® (plain) and Fospeg® (PEGylated)	[161]
Murine carcinomas: 4T1 murine (breast), CT26 (colon) and B16-F10 (skin)	0.5–1 x10 ⁶ cells grafted on day 10	N,N,N-trimethyl chitosan NPs loaded with IL-6 and STAT3 siRNA and surface coated with hyaluronate	[163]

to enhance the circulation lifetime of NPs and may subsequently result in improved tumor accumulation due to the enhanced permeability and retention (EPR) effect. PEGylated NPs also avoid rapid clearance and the adsorption of unwanted proteins (*i.e.* formation of ‘protein corona’), which can reduce the NP efficiency and make them vulnerable to

opsonization by the mononuclear phagocyte system [129,130].

Various functional groups can also alter the overall NP surface charge and modulate the formation of protein corona and opsonization. Lunov *et al.* [131] demonstrated that polystyrene (PS) NPs surface decorated with carboxylic acid (PS-COOH) or amine

(PS-NH₂) were distinctively uptaken by different cell types. While PS-COOH was preferentially found in macrophages in 2D cell culture and in the liver of chicken embryo during CAM assay due to the involvement of the reticuloendothelial system in the excretion of foreign materials, PS-NH₂ was mostly detected in the tumor grafts [131]. The group further demonstrated the advantage of PS-NH₂ in terms of suppressing neovascularization in leukemia tumor xenografts. The presence of the amine group caused swelling and degradation of the lysosomes, and inhibited the activities of mammalian target of rapamycin (mTOR) proliferation-promoting kinase [132]. Although leukemia is not a solid tumor, the CAM may still provide an alternative biological model to investigate vascularization and the effects of candidate drugs on angiogenesis, which are also crucial in hematological malignancies [133,134].

Surface functionalization with targeting moieties for selective nano-delivery is an extensively explored approach to improve NP accumulation in tumors [135]. In this regard, the folate receptor is one of the common membrane-associated targets that is also proposed to aid in overcoming multidrug resistance [135,136]. In one study, cancer cells highly expressing the alpha isomer of the folate receptor (FR- α) were

targeted using folic acid-decorated silica NPs. The NPs were also loaded with a γ -secretase inhibitor (GSI) and administered topically or intravenously on tumor-grafted CAMs. The uptake of NPs in MDA-MB-231 breast tumors was higher than in PC3 prostate tumors, consistent with the undetected expression of FR- α in PC3 cells. Furthermore, a decreased Ki67 expression was seen in breast tumor grafts after NP treatment, indicating the anti-proliferative effects of the nanoformulation [50]. Meanwhile, Steinmetz *et al.* [137] developed a cowpea mosaic virus-derived NPs to targeting gastrin-releasing peptide receptors in prostate cancer. A fluorophore was incorporated to track the accumulation, penetration, and retention of the NPs in green fluorescent protein (GFP)-expressing PC3 tumors grafts (Figure 4d). The functionalized viral NPs selectively accumulated in the tumors 1 h after injection and were retained for at least 6 h [137]. Conversely, some functional groups utilized as targeting moieties can in themselves elicit an antitumor action. Working with this approach, Niemelä *et al.* [138] functionalized the surface of silica NPs with the folate antagonist methotrexate, and loaded the inner NP cavity with fingolimod, which blocks the production of tumor-promoting sphingolipid

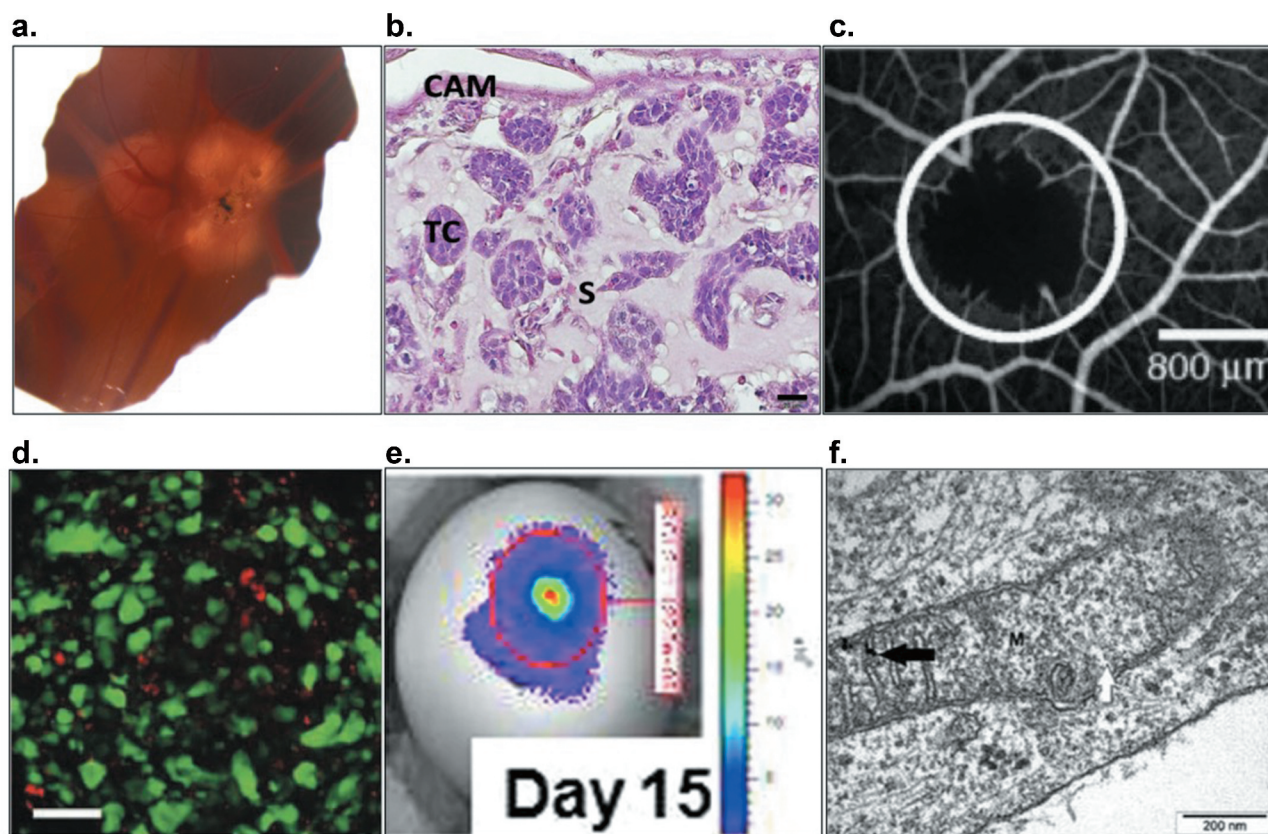


Figure 4. Various imaging technologies are compatibly employed to monitor and analyze the tumor and vascular networks. (a) Suit2.28 wt pancreatic carcinoma imaged 7 days after grafting using stereomicroscope (unpublished data). (b) Harvested tumor of UPCI:SCC-154 head and neck squamous cell carcinoma stained with H&E (TC = tumor cells; S = stroma; scale bar = 20 μ m; unpublished data). (c) Vascular occlusion following PDT imaged through fluorescence angiography. Reproduced with permission from Vargis *et al.* [171]. Copyright 2007 by Elsevier B.V. (d) Fluorescence immunohistochemistry of prostate tumor section, demonstrating the accumulation and penetration of viral nanoparticles (green = GFP-expressing PC-3 cells; red = viral NPs; scale bar = 75 μ m). Reproduced with permission from Steinmetz *et al.* [137]. Copyright 2011 by WILEY-VCH Verlag GmbH & Co. KGaA, Weinheim. (e) Bioluminescence intensity of Fluc-mCherry PDAC tumors at 15 days after grafting. Adapted from Rovithi *et al.* [11]. Copyright 2017 by the authors (f) TEM image depicting a mitochondrion (m) of glioma tumor incubated with platinum nanoparticles (black arrows; scale bar = 200 nm). Reproduced from Kutwin *et al.* [149]. Copyright 2016 by Termedia & Banach.

sphingosine 1-phosphate. The delivery of the drug cocktail promoted necrosis and reduced the invasiveness of thyroid carcinoma grafted on CAM [138].

2.3.2. NMs for tumor imaging

Tumors grafted on CAMs can also be conveniently used to evaluate materials specifically fabricated for disease imaging. Technologies currently used in clinics, which are also subjects for NM applications, may benefit from the availability of CAM tumor models for rapid evaluation and tailor fitting. For instance in MRI, there is a persisting need to develop effective and safe contrast agents as the commonly employed gadolinium (III) complexes have sub-optimal efficiencies and may pose severe side effects [139]. In this regard, the imaging efficiency of cHSA-PEO(2000)₁₆-Gd, an albumin-conjugated polymeric nanoformulation, was compared to Gadofosveset, a Gd-DOTA complex clinically used as MRI contrast agent, using breast cancer-grafted CAMs. Evaluations were performed 16 days after embryo incubation to take advantage of the mature blood vessels and maximum blood volume (~3 mL) in the avian system. Intravenous administration of NPs resulted in increased tumor uptake and longer retention lasting for 40 h post-injection [140]. In contrast, Faucher and coworkers [141] utilized glioblastoma cells that were incubated with ultrasmall gadolinium oxide (Gd₂O₃) NPs prior to grafting. The labeled cells were visible even without image post-processing and Gd₂O₃ NPs did not introduce dramatic changes in tumor weight [141].

Alternatively, nano-encapsulation can be implemented to improve the photostability of fluorophores and enhance the resulting fluorescence imaging. In this respect, a gelatin-conjugated cyanine derivative was encapsulated in iron oxide NPs functionalized with peanut agglutinin or anti-carcinoembryonic antigen (αCEA) antibody to target the Thomsen-Friedenreich antigen and CEA. Nano-encapsulation protected the fluorophore from photobleaching, as shown with the stable fluorescence intensity in comparison to cyanine in buffered solution [142]. Nano-encapsulation can also improve the biocompatibility of hydrophobic imaging contrast agents. For example, polylactic acid NPs have been developed to encapsulate hypericin, a nature-derived molecule extracted from *Hypericum perforatum* with potential applications in photodetection and photodynamic therapy (PDT) [143]. Aqueous solutions of hypericin-loaded NPs were administered intravenously to ovarian tumor systems. The encapsulation led to an enhanced tumor fluorescence intensity and reduced vascular leakage of the contrast agent [144].

Certain types of NMs have innate optical properties compatible with imaging applications. Among which are upconversion nanoparticles (UCNPs), which can convert near-infrared (NIR) radiation into visible light through two- or multiphoton optical phenomena [145]. These NPs are doped with rare earth elements such as lanthanide (La), erbium (Er), and ytterbium (Yb), and offer deep tissue imaging due to the use of NIR radiation. UCNP-facilitated imaging also presents good sensitivity, photostability, and low toxicity [146]. Yb- and Er-

containing UCNPs were exploited in the detection of small tumors and real-time imaging of blood vessels, tumors, and surrounding tissues. The NPs were also conjugated with estrogen receptor-α mAb, to actively target small breast cancer spheroids (diameter ~500 μm) grafted on the CAM. The target-labeled UCNPs selectively accumulated in the tumor xenograft while signals from unlabeled UCNPs were also detected on the surrounding tissue of the tumor [47].

2.3.3. NM toxicity

Some types of NMs possess intrinsic properties that can induce antitumor effects. This has been demonstrated using ultradispersed detonation diamonds and microwave-radiofrequency carbon allotrope NPs, which caused tumor size and weight reductions on U87 glioblastoma xenografts. Expression of fibroblast growth factor (FGF-2) and VEGF was lower in the treated tumors compared to the untreated controls [147]. Another study also utilized glioblastoma-grafted CAMs to probe the effects of silver NPs, in which lower proliferation and mitotic indices were recorded in comparison to both the control and tumors treated solely with the vehicle solution. Accompanying protein analyses revealed elevated expressions of caspase 9 and caspase 3 in tumors exposed to the NPs, demonstrating the pro-apoptotic effects of the Ag NPs [148]. Glioblastoma-grafted CAMs were also employed to compare the anticancer effects of cisplatin and platinum NPs, in order to further understand the mechanism by which Pt NPs may induce an effect given their different physical and chemical properties in comparison to chemotherapeutic Pt (II) complexes. Indeed, Pt NPs caused reductions in tumor volumes and weights that were mainly attributed to their interaction with the mitochondria (Figure 4(f)), and the propensity to upregulate the mRNA expressions of the pro-apoptotic molecule caspase-3 and tumor suppressor p53 [149].

CAM tumor models have also been employed to evaluate the carcinogenic effects of NMs. This is also an important concern, considering the increasing manufacturing and rate of usage of NMs for various applications. The pro-angiogenic properties of hybrid material tungsten carbide cobalt (WC-Co) NPs were investigated using CAMs grafted with lung adenocarcinoma and contrasted with human bronchial epithelial cell xenografts. Enhanced blood vessel formation was observed on both the tumor and normal tissue, accompanied by increased expression and activation of angiogenesis and inflammation-promoting markers like VEGF, nuclear factor kappa-light chain-enhancer of activated B cells (NF-κB), and Akt pathway. Hence, the study raised warnings on the potential carcinogenic hazards of nano-sized WC-Co, which has been known to cause pulmonary diseases [150].

2.3.4. NMs-facilitated treatment modalities

Several investigations on NMs focus on their prospective applications in cancer treatment. Similar to imaging contrast agents, nano-encapsulation presents an approach to improve drug pharmacokinetics and biocompatibility. Various NPs are developed and optimized for chemotherapy as these materials offer high

loading capacity, protection of the loaded molecule, prevention of premature leakage, and potentials for selective, triggered, and/or controlled payload release [151–154]. Following the successful clinical translation of Doxil® in 1995, doxorubicin was and remains as one of the most used model molecules for nanoencapsulation studies, also due to its intrinsic fluorescence that can be used for detection and quantification [155]. Nevertheless, studies are continuously performed to further improve the formulation of doxorubicin-loaded NPs, such as by varying the NP synthesis materials and properties. For instance, doxorubicin was loaded in silica NPs with varied pore sizes, with the final loading efficiency ranging from 20% to 50% w/w (%drug/NP). A general increase in antitumor activity was observed with doxorubicin-loaded NPs in comparison to the free drug solution. Meanwhile, the fluorescence of doxorubicin was utilized to monitor the accumulation of NPs in OVCAR-8 tumors and the biodistribution in the off-target organs of the chicken embryo. Remarkably, doxorubicin administered to the models in free solution was detected in various organs of the embryo [156].

Usually, the mechanisms of action of free and NP-incorporated drugs must be compared to identify whether the encapsulation procedure has caused functional alterations. In line with this, Yalcin and coworkers [157] demonstrated that tetraiodothyroacetic acid (Tetrac), a thyroid hormone antagonist, and its polymeric NP formulation (poly(lactic-co-glycolic acid)-Tetrac or PLGA-Tetrac) were both efficient in inhibiting cell proliferation and angiogenesis. In its free form, Tetrac elicits effects initiated either in the plasma membrane through the $\alpha\beta_3$ integrin or in the nucleus through the nuclear thyroid hormone receptor. Fluorescence imaging confirmed the localization of the NPs on the cell membrane, while Tetrac in free solution was also able to reach the nucleus. Nevertheless, the comparable effects of the two treatments in CAM tumors supported the hypothesis that the free drug and the NPs mainly act on the plasma membrane of the renal cancer cells [157].

Other drugs are instead designed to interfere with vascular development. In the study of Paris *et al.* [158], the anti-angiogenic drug doxycycline was loaded together with a vascular disrupting agent fosbretabulin in mesoporous silica NPs. The NPs also contained gold nanorods for photothermal therapy and indocyanine green for PDT. The multimodal nanosystem restrained the formation of blood vessels surrounding the tumors and laser irradiation at 808 nm caused evident blood vessel damages with apparent hemorrhage [158].

Simultaneous delivery of multiple molecular cargos has also been attempted to construct nanoplatforams for theranostics (diagnosis + therapy). For instance, the nanoparticle albumin-bound (nab) technology was utilized to formulate dcHSA-Gd-Dox, which contained doxorubicin and Gd (III)-DOTA for MRI. The oncological relevance of nab-technology has been further raised with the clinical approval of Abraxane®, a paclitaxel nab-formulation first approved by the Food and Drug Administration in 2005 for metastatic breast cancer [159]. Imaging of breast cancer-grafted CAMs illustrated the tumor accumulation of dcHSA-Gd-Dox, which also demonstrated a better signal-to-noise ratio with respect to the standard Gd-

based MRI contrast agent MultiHance®. Meanwhile, the nanoencapsulation of doxorubicin improved the overall survival rate of the embryos compared to the models treated with doxorubicin in free solution. Attenuated cancer cell proliferation and enhanced apoptosis were also observed on NP-treated tumor xenografts [160].

The role of NPs in antitumor molecule delivery is further extended to PDT. In this treatment modality, photosensitizers (PS) are irradiated at specific wavelengths to generate cytotoxic reactive oxygen species. Likewise, PS encapsulation is performed to improve its stability, systemic circulation, tumor delivery, and to prevent off-target sensitization. Meta-tetra(hydroxyphenyl)chlorin (mTHPC) is a PS that has been approved for clinical applications in the European Union. Two liposomal formulations of mTHPC are available: the plain Foslip® and the PEGylated Fospeg®. These nanoformulations were compared on CAMs grafted with murine mammary carcinoma cells at different drug-light interval (DLI) periods, *i.e.* the time between the PS administration and light irradiation. It was observed that at a DLI of 1 h, tumor accumulation and PDT-induced antitumor effects in terms of necrosis area were better with Fospeg® than Foslip®. Additionally, Fospeg® was found to be less destructive on normal vasculatures [161].

Finally, gene delivery may also take advantage of NP-mediated delivery to avoid the complications with viral vectors, such as activation of the host's immune system and very limited payload capacity [162]. On this point, Masjedi and colleagues [163] utilized modified chitosan-based NPs to encapsulate siRNAs suppressing interleukin-6 and signal transducer and activator of transcription 3. These mechanisms support tumor progression by promoting proliferation, anti-apoptotic factors, and drug resistance. Treatment of CAMs grafted with murine cancer cells with the siRNA-loaded NPs resulted in reduced tumor size, weight, and number of blood microvessels. Furthermore, mRNA expressions of tumor and angiogenesis promoting genes FGF, transforming growth factor- β (TGF- β), and VEGF were downregulated [163].

3. CAM tumor model analysis: monitoring and end-point assays

Appropriate instruments and methodologies for monitoring the changes in the tumor system are fundamental in deriving information from CAM tumor models. In general, imaging and molecular detection assays are complementarily used to track the dynamics within the tumor system, and examine the consequent effects of treatment administration [14,34]. Imaging technologies enable real-time, rapid, qualitative, and (semi-) quantitative monitoring, while molecular identification and quantification assays allow detection with improved sensitivity and selectivity that could also allow investigations on genomic expression levels.

This section discusses the strategies commonly employed for the monitoring and analysis of CAM tumor models, focusing on documentations of the tumor features through imaging, and sensitive molecular detection of tumor-specific markers and administered therapeutics through various (bio)

molecular techniques. However, it should also be noted that analyses could be reasonably straightforward. Simple tools, such as rulers or calipers, may also be used to follow the changes in tumor features, and to document changes in sizes of the tumor or blood vessels. Other parameters do not require special instruments, as in the case of monitoring embryo vitality, which can be useful for drug (dosage) toxicity analyses, or tumor-grafting rate. Features and weights of harvested tumors may represent the ability of cancer cell lines or xenografts to grow and form solid tumors. Additionally, comparison of these features across different treatments and within different stages of embryonic development may infer treatment-driven effects.

3.1. Imaging of the tumor and vascular networks

As frequently reported, one of the advantages of CAM tumor models is the accessibility of the tumor and the blood vessels, which enables them to be straightforwardly observed and followed through various microscopy technologies (Figure 4) [34]. Bright field microscopes, most notably stereomicroscopes, are frequently used to monitor the condition and changes in the physical features of the tumor and blood vessels (Figure 4(a)), in which their dimensions and the extent of vascularization are regularly documented [37]. Functional blood vessels can be rapidly visualized using India ink and benzyl benzoate benzyl acid [68,164]. The measurements are often processed to derived parameters such as tumor volume [11,90] and relative vessel length [37,44], which are correlated to defined variables like grafting time points and treatment administration. Moreover, vascular density, blood vessel length, diameter, and vessel branch points can be optically monitored to evaluate pro- or anti-angiogenic responses [165,166]. In some studies, a CAM region-of-interest may be directly treated with disks made from nitrocellulose membrane or Whatman® filter paper containing molecules that may regulate angiogenesis and inflammation [101,167]. The extent of convergence of the blood vessels toward the disk consequently infers the angiogenic influence of the examined molecule. Moreover, this method allows to count the number of CAM vessels and branch points around the implant by defining an angiogenesis scoring rubric [63]. Bright field microscopy is also extensively used for histological analyses of the harvested tumor and tissues from the embryo. Reagents such as hematoxylin and eosin (H&E; Figure 4(b)), or trichrome stains are applied to distinguish the cellular organelles and stromal components, and to evaluate the conditions of the tumor and TME after treatment [50,156,161].

In comparison to bright field microscopy, fluorescence microscopy renders images with increased sensitivity, specificity, and image resolution [168]. Slices of fixed tumor can be processed as for immunohistochemistry, and biomolecules specifically present in certain cell types or under a particular condition can be identified using reagents tagged with fluorescent probes. Some of these commonly utilized fluorophore-tagged or probe-detected biomarkers include desmin for the vascularization [132], vimentin for stromal cells [156], Ki67 for

proliferation [44], terminal deoxynucleotidyl transferase (Tdt)-mediated dUTP nick-end labeling (TUNEL) for DNA fragmentation [160], tumor type-specific antibodies [49,92,138], or avian-specific markers [131]. Meanwhile, blood vessels can be visualized using fluorophore-conjugated dextran [169]. Varied molecular weights of fluorescent dextran have also been utilized to study molecular diffusion, kinetics, and vascular permeability, which can be valuable in analyzing drug pharmacokinetics [34,169]. Alternatively, *Lens culinaris* agglutinin can be used in imaging the blood vessels, as lectins like agglutinins specifically bind to avian endothelial cells in blood vessels [15,49,170]. Fluorophores like rhodamine derivatives have also been used for angiographies, when examining vascular injury following PDT (Figure 4(c)) [151,171]. Furthermore, PDT-induced vascular occlusion can be visualized and then assessed using scoring systems corresponding to the extent of vascular re-growth and branching after triggering the action of the photosensitizer through light irradiation [161,171]. Attaching fluorophores to human or avian-specific endothelial markers may give information on blood vessel origin. This has been demonstrated using CD31 and *Sambucus nigra* lectins to distinguish human and chick blood vessels, respectively, with the samples also labelled with anti-desmin to mark blood vessels regardless of origin. This methodology allowed visual assessments of the efficiency of the integration of chick host vascularization, the preservation of intratumoral vessels from the excised tissue sample, and vascular anastomosis [68].

Fluorescence imaging is also vital in detecting the presence, tissue penetration, and biodistribution of naturally fluorescent materials or fluorophore-labeled nanomaterials within the tumor (Figure 4(d)), TME, and chick embryo organs [47,128,137,144,156]. To further facilitate the localization of fluorescent materials within a tumor mass, cells can be incubated with fluorescent organelle markers for simultaneous visualization [125]. Otherwise, cells can be genetically engineered prior to grafting such that they express reporter molecules like GFP and firefly luciferase that are detectable via fluorescence or luminescence [11,96,156,160]. Bioluminescence imaging (BLI) can then enable specific detection and quantitative monitoring of the engineered tumors over the course of the CAM assay (Figure 4(e)) [11,96]. This strategy eases the monitoring of tumor growth or shrinkage under given conditions, is applicable to examine tumor migration and metastasis, and can be coupled with *in vivo* imaging systems for real-time and unperturbed monitoring [15]. Alternatively, fluorophores are utilized in fluorescence-activated cell sorting to label specific population of cells, such as cancer stem cells present in the tumor, and compare relative to another tumor feature (e.g. tumor mass) [172]. Recorded images can be further processed using software programs dedicated to analyze various conditions, among which are Volocity® for fluorescent 3D renders, and DCI HetCAM software for vascular branching [37,44,137,173]. High-resolution image stacks may also be acquired by taking advantage of advanced fluorescence microscopes such as spinning disk confocal microscope, which simultaneously takes images from multiple points and is therefore suitable for 3D imaging

of live samples [128,174,175]. Imaging-facilitated (semi-) quantification of circulating and metastasizing cancer cell is possible with intravital video-microscopy [59]. This method takes advantage of an inverted microscope with oblique transillumination to acquire high-resolution images of the microvasculature, along with fluorescence features to detect labeled cancer cells. However, this method can only observe a superficial layer of tissue with thickness of up to 50 μm [176].

In situ hybridization (ISH) is a sensitive biomolecular technique in which targeted DNA or RNA sequences are detected through complementary sequences labeled with reporter probes [177]. Integrating the principle of hybridization with imaging instruments has various applications in CAM tumor studies. For instance, ISH has been used to confirm the integrity of CAM tumors with a known characteristic of that tumor type, such as the presence of viral oncogene [93]. Furthermore, specific genes involved in the development of endothelial cells in different embryonic tissues at various days of development have been correlated through ISH [178]. The genetic probes can also be designed to selectively bind to tissues of human or avian origin [49].

Further information on cellular ultra-structures can be deduced using electron microscopy. For example,

transmission electron microscopy may demonstrate the conditions of the cellular organelles and the TME, and can additionally locate the administered nanomaterials (Figure 4(f)) [92,149]. In certain cases, technologies evaluated on CAM tumor models are specifically developed for tumor imaging. Thus, tumor growth and other features of the embryo are monitored and visualized, for instance using MRI [140,160], MRI/PET [97], and PET/CT [98] (Figure 3).

3.2. Molecular detection and quantification

Integrating biomolecular markers into various imaging techniques has enabled visualization of tissues with increased specificity. Nevertheless, certain investigations are unfeasible with imaging alone and, thus, require more sensitive and quantitative methodologies that have been precisely established for molecular detection and measurement. This is the case with studying metastasis in CAM tumor models, as the limited experimentation period makes it difficult to observe macroscopic growth of tumor in secondary tumor site. Hence, procedures capable of specifically and sensitively detecting human tumor markers from the avian biological system are necessary to carry out micrometastasis analysis [58]. Among

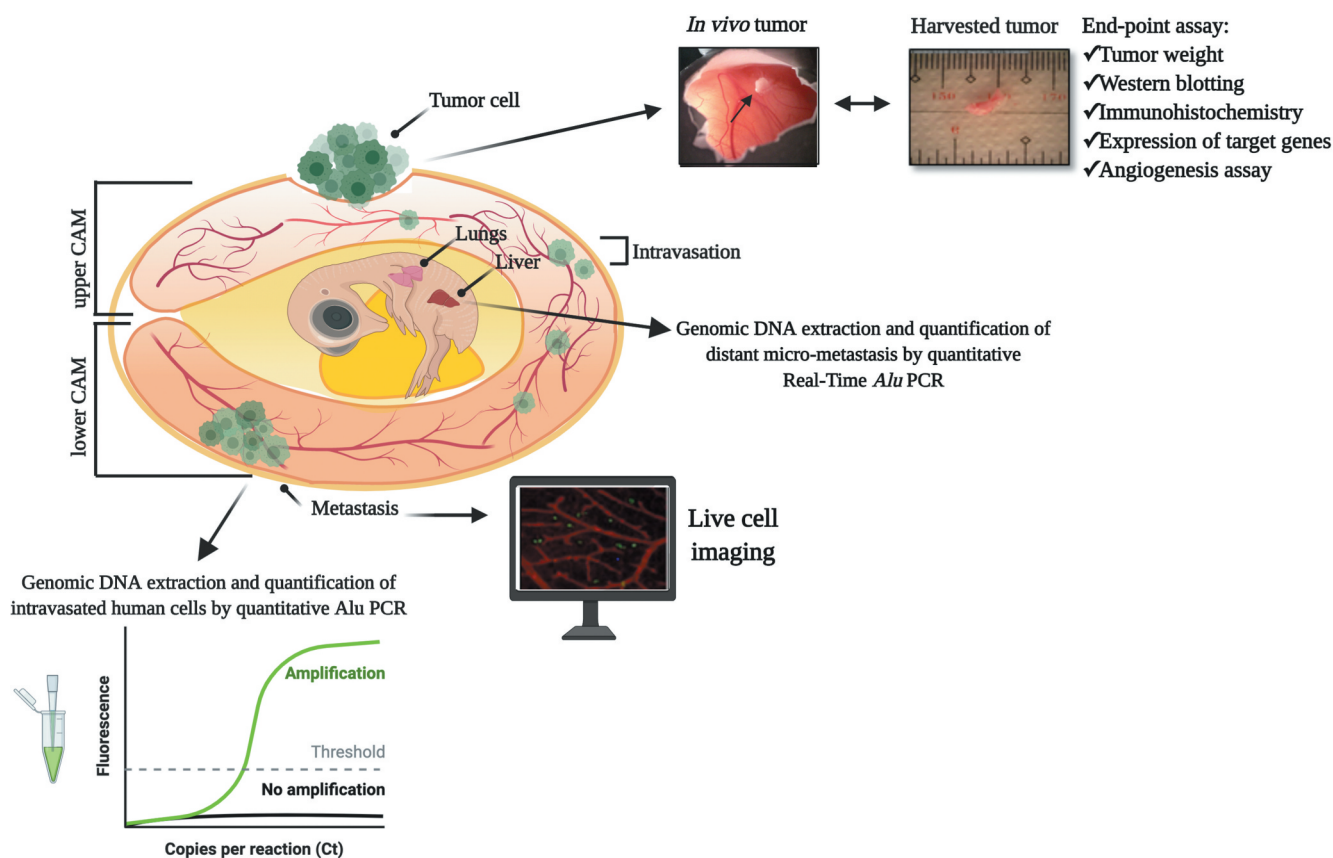


Figure 5. Overview of the chick embryo metastasis analysis. Fluorescently labeled cancer cells are engrafted on the upper CAM of the chick embryo. Several days of incubation allow the formation of a tumor mass. Then, invasive tumor cells start to intravasate and reach distal sites from the primary tumor region, such as in the lower CAM and the chick organs (e.g. liver, lungs). Metastasis can be detected and confirmed through PCR detection of human-specific Alu repeats, and live-cell imaging.

the human-specific markers significantly utilized in detecting cancer cells disseminated from the primary tumor site are *Alu* DNA repeats. These short interspersed nuclear elements are ubiquitously found in the human genome, and have been taken advantage in identifying human cells introduced in other non-primate organisms [179]. Detecting *Alu* repeats through polymerase chain reaction (PCR) on various tissues within the CAM tumor system provides a highly sensitive method to monitor the behaviors of cancer cell (Figure 5) [57,58]. It is important to note that while PCR can amplify genetic materials from both whole live cells and phagocytized cell debris, performing the quantification while the immune system of the chick embryo is still underdeveloped ensures that the data are indeed mainly due to viable cancer cells [57]. Additionally, time-correlated PCR-based *Alu* sequence detection has been essential in determining key steps that cause differential metastatic kinetics and efficiencies across various cancer cell lines [57,58,73]. Furthering *Alu* DNA repeats detection through real-time PCR resulted in the establishment of a sensitive method to detect as few as 25 cancer cells in an embryo's lung, with a wide linear range from 50 to 1×10^5 cells/lung [58]. On the other hand, chicken repeat 1 (CR1) can instead be used as the host-specific marker, as it is the main [long] interspersed repeat element in the chicken genome [43,49].

Real-time PCR may also be utilized to study gene expression regulation, which is significant in demonstrating the validity of CAM tumor system as an oncological model. Comparing the gene expression of key angiogenic and tumorigenic markers has shown its reliability in representing tumor behaviors that are similarly observed in patient-derived biopsies [11,90]. Similarly, up- or downregulation of human or chicken-specific genes can be followed throughout the embryonic developmental stages to identify pathways or mechanisms that may drive the tumor or vascular development [68,178]. PCR has also been valuable in distinguishing effects of certain experimental conditions at the genomic level. For instance, the expression of stromal genes between normal and tumor-grafted CAMs was compared to determine whether these can be correlated to normal embryonic developmental dynamics or to tumor growth [88]. Alterations in genomic expressions are also evaluated to investigate the effects and efficiency of therapeutics, by considering genes that influence angiogenesis, tumor suppression, cell proliferation, and apoptosis [11,91,147,149]. Accordingly, mRNAs that are commonly studied include sequences encoding for VEGF and FGF-2 for angiogenesis [70,147], p53 for tumor suppression [149], proliferating cell nuclear antigen (PCNA) for proliferation [149], and caspase-3 for apoptosis [149].

Other studies have instead analyzed proteins that likewise play vital roles in angiogenesis and tumorigenesis. This strategy has been applied in tracking the effects of therapeutics in controlling tumor-promoting or suppressing mechanisms that were reflected, for example, in the presence of growth factor receptors [180] or caspase apoptosis molecules [148]. Meanwhile, the gelatin zymography assay has been used to assess the expression and the activity of the gelatinase

enzymes in many malignant human tumor owing to the consistent association of MMPs and plasminogen activators with tumor cell migration and metastatic dissemination [181]. In this assay, cells are grown in fetal bovine serum (FBS)-containing medium until they reach 70–80% confluency, then the medium is replaced with FBS-free medium. After a determined period of growth in the FBS-free media, the conditioned medium is collected and it is prepared to run across a polyacrylamide gel with gelatin in electrophoresis. If MMP-2 or MMP-9 is present in the samples, the gelatin will be digested by the enzyme, resulting in clear bands of the active proteinases after staining with Coomassie Blue and destaining with methanol [57].

Pharmacokinetic behaviors and fate of administered therapeutics within the tumor system also need to be determined to further ascertain their efficiency. Hyphenated analytical instruments, such as liquid chromatography-mass spectrometry (LC-MS) for organic analytes and inductively coupled plasma-mass spectrometry (ICP-MS) for elemental analysis, could be used to monitor the behavior of administered molecules within the circulation [182], or measure the intratumoral concentration of chemotherapeutic drugs [44,183]. Furthermore, harvesting the organs of the embryo and subjecting to molecular quantitative analysis may provide insights on microsystemic bio-distribution [160,184].

4. Conclusion

In conclusion, the CAM as a platform for precision medicine could provide an alternative step in translational cancer research to assess experimental and novel strategies for both diagnostic and therapeutic purposes (*i.e.*, cancer theranostics), keeping in line with the 3Rs of experimental animal use. Although long-term effects cannot be evaluated in these models, crucial data about initial efficacy and potential toxicity on the organs of chemo/radio-treatments, as well as *in ovo* biodistribution of small molecules and nanomaterials could be acquired upon initial screening. Furthermore, the significance of CAMs as an *in vivo* model has been convincingly demonstrated, even if recapitulation of the human TME for cancer research remains a point of improvement. Additional studies to include more cellular components relevant to the human TME are suggested. Similarly, the technological advances and the decreasing costs of multi-omics platforms (including analysis of genome, transcriptome, proteome, lipidome, and metabolome) will enable profiling of CAM molecular features at different levels, providing the opportunity to exploit these models for the rational development of new cancer therapeutics.

5. Expert opinion

We reviewed an extensive list of applications of the CAM model, as an alternative to conventional animal models for preclinical (cancer) research. The rapid formation and accessibility for handling of patient-derived tumors in a well-vascularized *in vivo* model are two

main advantages of the CAM, however, several previously listed limitations support the use of a different *in vivo* model when investigating specific conditions. Observations of acute toxicity and short-term effects of IR-induced DNA damage conform to the timeframe of experimental use of the CAM are only within the order of days. Instead, other animal models, such as mice, might be more suitable to study long-term effects and acquired resistance against pharmacological, radiotherapeutic, or combination treatment. Grafting conditioned cell lines against the treatment of interest could be a strategy to overcome this limitation [106].

Aside from the practical aspects, other limitations could demonstrate the CAM to be less suitable as an *in vivo* model. Firstly, an important implication is related to the vascularization of xenografts. While several types of human tumors, such as gliomas, are known to be highly vascularized in patients, this might not always be the case. Pancreatic cancer, for example, is well-known for its stromal density and in reality, is poorly vascularized [185]. Moreover, the influence of the TME has increasingly become a clinically relevant element [186]. A description of the composition of the vasculature and stroma of the CAM is thus of profound importance. To the best of our knowledge, only one proteomic analysis of the CAM was performed in context of human glioblastoma, where authors identified differentially expressed proteins between tumor-bearing CAM and wounded CAM for potential target finding [187]. Certainly, the CAM contains various ECM proteins such as fibronectin, collagen I and IV, laminin, and integrins which are similarly found in humans [188]. Moreover, the composition of these ECM proteins changes as the CAM develops over time and might differ due to interspecies differences [189]. Naturally, further studies are required for validation of potential interactions between the ECM proteins and tumor cells. Nevertheless, the CAM provides a very accessible and natural immune-deficient environment from the start as an *in vivo* model. While other conventional animal models, like mice, have to be immune-deficient in order to facilitate tumor xenograft formation.

Secondly, aside from ECM proteins, the TME also contains several cellular components, including cancer-associated fibroblasts that could assist tumor growth and invasion via paracrine signaling [190]. In an attempt to recapitulate the clinical setting, Schneiderhan *et al.* [191] managed to co-graft PANC-1 cells and pancreatic stellate cells, in which the latter are well-known to produce and secrete ECM proteins. As hypothesized, they showed via H&E staining that the presence of pancreatic stellate cells increased tumor invasion and had markedly increased tumor weight. More studies are warranted to identify important cellular aspects of the TME and the differences and similarities of the CAM in comparison to the human-derived microenvironment.

Despite these limitations, the CAM offers a unique platform to assess initial effect(s) of therapeutic interventions, including novel experimental compounds, nanomaterials, chemoradiotherapy, and hyperthermia combinations. The model could be utilized as a translational step in preclinical studies,

prior to commitment of more cumbersome and expensive *in vivo* studies. Future investigations should focus on comparison studies for human and avian similarities or discrepancies in order to take the differences into account for interpretation of data. However, the characterization of the chick embryo genome and the development of specific antibodies for blood and lymphatic endothelial cells and stroma components, as well as recent studies suggesting potential applications of gene editing in chickens [192,193] will help to better characterize the interactions between implanted human tissues and chicken tissues.

Acknowledgments

The authors would like to thank Ms. Kitty Castricum for images on Suit2.28wt, Dr. Claudia Kusmic, and Ms. Sabrina Marchetti for the UPCI: SCC-154 H&E image.

Figures 1(c), 2(a), 2c, and 5 were created with BioRender.com. Permissions were obtained for the following reproduced figures: Figure 1(a) = Adapted from Romanoff (Cornell Rural School Leaflet) [12] and Smith [13]. Copyright 2019 by the Mississippi State University Extension Service; Figure 2(d) = Reproduced with permission from Deryugina and Kiosses [81]. Copyright 2017 by the authors; Figure 4(a) = Reproduced from Warnock *et al.* [98]. Copyright 2013 by the Society of Nuclear Medicine and Molecular Imaging, Inc.; Figure 3(b) = Reproduced from Winter *et al.* [99]. Copyright 2020 by the authors; Figure 4(c) = Reproduced with permission from Vargas *et al.* [171]. Copyright 2007 by Elsevier B.V.; Figure 4(d) = Reproduced with permission from Steinmetz *et al.* [137]. Copyright 2011 by WILEY-VCH Verlag GmbH & Co. KGaA, Weinheim; Figure 4(e) = Adapted from Rovithi *et al.* [11]. Copyright 2017 by the authors; Figure 4F = Reproduced from Kutwin *et al.* [149]. Copyright 2016 by Termedia & Banach.

Declaration of interest

The authors have no relevant affiliations or financial involvement with any organization or entity with a financial interest in or financial conflict with the subject matter or materials discussed in the manuscript. This includes employment, consultancies, honoraria, stock ownership or options, expert testimony, grants or patents received or pending, or royalties.

Reviewer disclosures

Peer reviewers on this manuscript have no relevant financial or other relationships to disclose.

Funding

This work was supported by Associazione Italiana per la Ricerca sul Cancro (AIRC) under MFAG 2017 – ID 19852 project – P.I. Voliani Valerio, AIRC Start-Up #14422 project – P.I. Elisa Giovannetti, and Zabawas Foundation/Cancer Center Amsterdam (CCA) project #2006784 – P.I. Peter Sminia.

ORCID

Valerio Voliani  <http://orcid.org/0000-0003-1311-3349>

References

Papers of special note have been highlighted as either of interest (*) or of considerable interest (**) to readers.

1. Antoni D, Burckel H, Josset E, et al. Culture: a breakthrough in vivo. *Int J Mol Sci.* 2015;16(3):5517–5527.

2. Hirschhaeuser F, Menne H, Dittfeld C, et al. Multicellular tumor spheroids: an underestimated tool is catching up again. *J Biotechnol*. 2010;148(1):3–15.
3. Nath S, Devi GR. Three-dimensional culture systems in cancer research: focus on tumor spheroid model. *Pharmacol Ther*. 2016;163:94–108.
4. European Parliament. Directive 2010/63/EU - On the protection of animals used for scientific purposes <https://eur-lex.europa.eu/eli/dir/2010/63/oj>.
5. Tannenbaum J, Bennett BT. Russell and Burch's 3Rs then and now: the need for clarity in definition and purpose. *J Am Assoc Lab Anim Sci*. 2015;54(2):120–132.
6. Mapanao AK, Santi M, Combined Chemo-Photothermal VV. Treatment of three-dimensional head and neck squamous cell carcinomas by gold nano-architectures. *J Colloid Interface Sci*. 2021;582:1003–1011.
7. de Kruijff RM, van der Meer AJGM, Windmeijer CAA, et al. The therapeutic potential of polymersomes loaded with 225Ac evaluated in 2D and 3D in vitro glioma models. *Eur J Pharm Biopharm*. 2018 (Oct 2017);127:85–91.
8. Cassano D, Santi M, D'Autilia F, et al. Photothermal effect by NIR-responsive excretable ultrasmall-in-nano architectures. *Mater Horizons*. 2019;6(3):531–537.
9. Mapanao AK, Voliani, V. Three-dimensional tumor models: promoting Breakthroughs in nanotheranostics translational research. *Appl Mater Today*. 2020;19:100552.
10. Mangir N, Raza A, Haycock JW, et al. An improved in vivo methodology to visualise tumour induced changes in vasculature using the chick chorionic allantoic membrane assay. *In Vivo (Brooklyn)*. 2018;32(3):461–472.
11. Rovithi M, Avan A, Funel N, et al. Development of bioluminescent Chick Chorioallantoic Membrane (CAM) models for primary pancreatic cancer cells: a platform for drug testing. *Sci Rep*. July 2016;2017(7):1–13.
12. Romanoff AL. From the egg to the chick. *Cornell Rural School Leaflet*. 1939;33(1):57–63.
 - **This study shows the possibilities of genetically engineered patient-derived pancreatic cancer cells to assess response against chemotherapeutic combination treatment via non-invasive bioluminescent imaging.**
13. Smith TWJ. The avian embryo. *Mississippi State University Extension Service*. 2019.
 - **Concise technical and practical information on the physiological development and handling of eggs during chick embryo incubation.**
14. Ribatti, D. The chick embryo chorioallantoic membrane as a model for tumor biology. *Exp Cell Res*. 2014;328(2):314–324.
15. Deryugina EI, Quigley JP. Chick embryo chorioallantoic membrane model systems to study and visualize human tumor cell metastasis. *Histochem Cell Biol*. 2008;130(6):1119–1130.
16. Ribatti, D. The chick embryo Chorioallantoic Membrane (CAM). A multifaceted experimental model. *Mech Dev*. 2016;141:70–77.
17. Gabrielli MG, Accili D. The Chick Chorioallantoic Membrane: a Model of Molecular, Structural, and Functional Adaptation to Transepithelial Ion Transport and Barrier Function during Embryonic Development. *J Biomed Biotechnol*. 2010;2010:940741.
18. Vargas A, Zeisser-Labouèbe M, Lange N, et al. The chick embryo and Its Chorioallantoic Membrane (CAM) for the in vivo evaluation of drug delivery systems. *Adv Drug Deliv Rev*. 2007;59(11):1162–1176.
 - **Comprehensive review on the application of tumor-grafted CAMs for drug delivery and pharmacological studies.**
19. Samkoe KS, Clancy AA, Karotki A, et al. Complete blood vessel occlusion in the chick chorioallantoic membrane using two-photon excitation photodynamic therapy: implications for treatment of wet age-related macular degeneration. *J Biomed Opt*. 2007;12(3):034025.
20. Ribatti D, Vacca A, Cantatore FP, et al. An experimental study in the chick embryo chorioallantoic membrane of the anti-angiogenic activity of cyclosporine in rheumatoid arthritis versus osteoarthritis. *Inflamm Res*. 2000;49(8):418–423.
21. Moreno-Jiménez I, Hulsart-Billstrom G, Lanham SA, Janeczek AA, Kontouli N, Kanczler JM, Evans ND, Oreffo ROC. The Chorioallantoic Membrane (CAM) assay for the study of human bone regeneration: a refinement animal model for tissue engineering. *Sci Rep*. 2016;6 (April): 1–12.
22. Fredrickson TN, Sechler JMG, Palumbo GJ, et al. Acute inflammatory response to cowpox virus infection of the chorioallantoic membrane of the chick embryo. *Virology*. 1992;187(2):693–704.
23. Ausprunk DH, Knighton DR, Folkman J. Vascularization of normal and neoplastic tissues grafted to the chick chorioallantoic role of host and preexisting graft blood vessels. *Am J Pathol*. 1975;79(3):597–618.
24. Hanahan D, Weinberg RA. Hallmarks of cancer: the next generation. *Cell*. 2011;646–674. DOI:10.1016/j.cell.2011.02.013.
25. El-Kenawi AE, El-Remessy AB. Angiogenesis inhibitors in cancer therapy: mechanistic perspective on classification and treatment rationales. *Br J Pharmacol*. 2013;170(4):712–729.
26. Berg EL, Hsu YC, Lee JA. Consideration of the cellular microenvironment: physiologically relevant co-culture systems in drug discovery. *Adv Drug Deliv Rev*. 2014;69–70:190–204.
27. Chiew GGY, Wei N, Sultania S, et al. Bioengineered three-dimensional co-culture of cancer cells and endothelial cells: a model system for dual analysis of tumor growth and angiogenesis. *Biotechnol Bioeng*. 2017;114(8):1865–1877.
28. van Duinen V, Trietsch SJ, Joore J, et al. Microfluidic 3D cell culture: from tools to tissue models. *Curr Opin Biotechnol*. 2015;35:118–126.
29. Sung KE, Beebe DJ. Microfluidic 3D models of cancer. *Adv Drug Deliv Rev*. 2014;79:68–78.
30. Albanese A, Lam AK, Sykes EA, et al. Tumour-on-a-chip provides an optical window into nanoparticle tissue transport. *Nat Commun*. 2013;4(1):2718.
31. Virumbrales-Muñoz M, Ayuso JM, Olave M, et al. Multiwell capillarity-based microfluidic device for the study of 3D tumour tissue-2D endothelium interactions and drug screening in co-culture models. *Sci Rep*. 2017;7(1):1–15.
32. Li W, Khan M, Mao S, et al. Advances in Tumor-Endothelial Cells Co-Culture and Interaction on Microfluidics. *J Pharm Anal*. 2018;8(4):210–218.
33. Comşa Ş, Ceauşu AR, Popescu R, et al. The MSC-MCF-7 duet playing tumor vasculogenesis and angiogenesis onto the chick embryo chorioallantoic membrane. *In Vivo (Brooklyn)*. 2020;34(6):3315–3325.
34. Nowak-Sliwinska P, Segura T, Iruela-Arispe ML. The chicken chorioallantoic membrane model in biology, medicine and bioengineering. *Angiogenesis*. 2014;17(4):779–804.
35. Janse EM, Jeurissen SHM. Ontogeny and function of two non-lymphoid cell populations in the chicken embryo. *Immunobiology*. 1991;182(5):472–481.
36. Dünker N, Jendrossek V. Implementation of the chick Chorioallantoic Membrane (CAM) model in radiation biology and experimental radiation oncology research. *Cancers (Basel)*. 2019;11(10):10.
37. Kleibecker EA, Schulkens IAE, Castricum KCM, et al. Examination of the role of galectins during in vivo angiogenesis using the chick chorioallantoic membrane assay. *Method Mol Biol*. 2015;1207:305–315.
38. National Institute of Health. The public health service responds to commonly asked questions. Cited Jan 5, 2021. <https://grants.nih.gov/grants/olaw/references/ilar91.htm>.
39. Campbell MLH, Mellor DJ, Sandoe P. How should the welfare of fetal and neurologically immature postnatal animals be protected? *Anim Welf*. 2014;23(4):369–379.

40. European Parliament. Directive 2010/63/EU of the European parliament and of the council of 22 September 2010 on the protection of animals used for scientific purposes. *Official J*, 2010, L276, 33–79. <https://eur-lex.europa.eu/legal-content/DE/TXT/PDF/?uri=CELEX:32010L0063&from=en> (accessed on Jan 13, 2021).
41. Hamburger V, Hamilton HLA. Series of normal stages in the development of the chick embryo. *J Morphol*. 1951;88(3):49–92.
42. Burt DW. Chicken genome: current status and future opportunities. *Genome Res*. 2005;15(12):1692–1698.
43. International Chicken Genome Sequencing Consortium. Sequence and comparative analysis of the chicken genome provide unique perspectives on vertebrate evolution. *Nature*. 2004;432(7018):695–716.
44. Kleibeuker EA, Ten Hooven MA, Castricum KC, et al. Optimal treatment scheduling of ionizing radiation and sunitinib improves the antitumor activity and allows dose reduction. *Cancer Med*. 2015;4(7):1003–1015.
45. Kue CS, Tan KY, Lam ML, et al. Chick embryo Chorioallantoic Membrane (CAM): an alternative predictive model in acute toxicological studies for anti-cancer drugs. *Exp Anim*. 2014;64(2):129–138.
46. Rous P, Murphy JB. Tumor implantations in the developing embryo. *J Am Med Assoc*. 1911;LVI(10):741.
47. Liu K, Holz JA, Ding Y, et al. Targeted labeling of an early-stage tumor spheroid in a chorioallantoic membrane model with upconversion nanoparticles. *Nanoscale*. 2015;7(5):1596–1600.
48. DeBord LC, Pathak RR, Villaneuva M, et al. The chick Chorioallantoic Membrane (CAM) as a versatile Patient-Derived Xenograft (PDX) platform for precision medicine and preclinical research. *Am J Cancer Res*. 1642–1660;2018(8):8.
49. Kunz P, Schenker A, Sähr H, et al. Optimization of the chicken chorioallantoic membrane assay as reliable in vivo model for the analysis of osteosarcoma. *PLoS One*. 2019;14(4):1–16.
- **Analytical validation and observation on the effects of practical grafting techniques on osteosarcoma tumor formation. Simultaneously used chicken CR1 and human *Alu* DNA repeats.**
50. Wittig R, Rosenholm JM, von Haartman E, et al. Active targeting of mesoporous silica drug carriers enhances γ -secretase inhibitor efficacy in an in vivo model for breast cancer. *Nanomedicine*. 2014;9(7):971–987.
- **This study demonstrates an analytical optimization of tumor grafting condition, in terms of making lesions and using varieties of Matrigel.**
51. Bakhomou SF, Ngo B, Laughney AM, et al. Chromosomal instability drives metastasis through a cytosolic DNA response. *Nature*. 2018;553(7689):467–472.
52. Bakhomou SF, Compton DA, Instability C. Cancer: a complex relationship with therapeutic potential. *J Clin Invest*. 2012;122(4):1138–1143.
53. Shlien A, Malkin D. Copy number variations and cancer. *Genome Med*. 2009;1(6):1–9.
54. Pantel K, Brakenhoff RH. Dissecting the metastatic cascade. *Nat Rev Cancer*. 2004;4(6):448–456.
55. Van Zijl F, Krupitza G, Mikulits W. Initial steps of metastasis: cell invasion and endothelial transmigration. *Mutat Res - Rev Mutat Res*. 2011;728(1–2):23–34.
56. Mierke CT. The matrix environmental and cell mechanical properties regulate cell migration and contribute to the invasive phenotype of cancer cells. *Reports Prog Phys*. 2019;82(6):6.
57. Kim J, Yu W, Kovalski K, et al. Requirement for specific proteases in cancer cell intravasation as revealed by a novel semiquantitative PCR-based assay. *Cell*. 1998;94(3):353–362.
58. Zijlstra A, Mellor R, Panzarella G, et al. Analysis of rate-limiting steps in the metastatic cascade using human-specific real-time polymerase chain reaction. *Cancer Res*. 2002;62(23):7083–7092.
- **One of the pioneer studies on combining the sensitivity of real time-PCR with the specificity of *Alu* sequences for monitoring the metastatic dissemination of human tumor cells in chick embryo.**
59. Koop S, Schmidt EE, Macdonald IC, et al. Independence of metastatic ability and extravasation: metastatic Ras-transformed and control fibroblasts extravasate equally well. *Proc Natl Acad Sci U S A*. 1996;93(20):11080–11084.
60. Bayless KJ, Johnson GA. Role of the cytoskeleton in formation and maintenance of angiogenic sprouts. *J Vasc Res*. 2011;48(5):369–385.
61. Patel-Hett S, D'Amore PA. Signal transduction in vasculogenesis and developmental angiogenesis. *Int J Dev Biol*. 2011;55(4–5):353–363.
62. Tonini T, Rossi F, Claudio PP. Molecular basis of angiogenesis and cancer. *Oncogene*. 2003;22(43):6549–6556.
63. Deryugina EI, Quigley JP. Chick embryo chorioallantoic membrane models to quantify angiogenesis induced by inflammatory and tumor cells or purified effector molecules. *Methods Enzymol*. 2008;444:21–41.
64. Knighton D, Ausprunk D, Tapper D, et al. Vascular phases of tumour growth in the chick embryo. *Br J Cancer*. 1977;35(3):347–356.
- **One of the earliest studies focusing on tumor formation on CAM, which highlighted the dynamics of vascular development in the xenografts.**
65. Nagy J, Chang S-H, Shih S-C, et al. Heterogeneity of the Tumor Vasculature. *Semin Thromb Hemost*. 2010;36(3):321–331.
66. Deryugina EI. Chorioallantoic membrane microtumor model to study the mechanisms of tumor angiogenesis, vascular permeability, and tumor cell intravasation. In: Martin S, Hewett P, editors. *In Angiogenesis Protocol*. Vol. 1430. Human Press: New York, NY; 2016. p. 283–298.
67. Benazzi C, Al-Dissi A, Chau CH, et al. Angiogenesis in spontaneous tumors and implications for comparative tumor biology. *Sci World J*. 2014;2014:1–16.
68. Fergelot P, Bernhard JC, Soulet F, et al. The experimental renal cell carcinoma model in the chick embryo. *Angiogenesis*. 2013;16(1):181–194.
69. Baum O, Suter F, Gerber B, et al. Angiogenesis in the developing chicken chorioallantoic membrane. *Microcirculation*. 2010;17(6):447–457.
70. Marinaccio C, Nico B, Ribatti D. Differential expression of angiogenic and anti-angiogenic molecules in the chick embryo chorioallantoic membrane and selected organs during embryonic development. *Int J Dev Biol*. 2013;57(11–12):907–916.
71. Plate KH, Breier G, Millauer B, et al. Up-regulation of vascular endothelial growth factor and its cognate receptors in a rat glioma model of tumor angiogenesis. *Cancer Res*. 1993;53(23):5822–5827.
72. Petruzzelli GJ, Johnson JT, Snyderman CH, et al. Angiogenesis induced by head and neck squamous cell carcinoma xenografts in the chick embryo chorioallantoic membrane model. *Ann Otol Rhinol Laryngol*. 1993;102(3):215–221.
73. Subauste MC, Kupriyanova TA, Conn EM, et al. Evaluation of metastatic and angiogenic potentials of human colon carcinoma cells in chick embryo model systems. *Clin Exp Metastasis*. 2009;26(8):1033–1047.
74. Sys G, Van Bockstal M, Forsyth R, et al. Tumor grafts derived from sarcoma patients retain tumor morphology, viability, and invasion potential and indicate disease outcomes in the chick chorioallantoic membrane model. *Cancer Lett*. 2012;326(1):69–78.
75. Klagsbrun M, Knighton D, Folkman J. Tumor angiogenesis activity in cells grown in tissue culture. *Cancer Res*. 1976;36(1):110–114.
- **Comparison of human glioblastoma and meningioma cell lines with patient-derived glioblastoma and meningioma to demonstrate significant differences in the angiogenic response upon grafting on CAM.**
76. Moscatelli D, Joseph-Silverstein J, Presta M, et al. Multiple forms of an angiogenesis factor: basic fibroblast growth factor. *Biochimie*. 1987;70(1):83–87.

77. Brem S, Cotran R, Tumor Angiogenesis FJ, et al. Method for histologic grading. *J Natl Cancer Inst.* **1972**;48(2):347–356.
78. Mostafa LK, Jones DB, Wright DH. Mechanism of the induction of angiogenesis by human neoplastic lymphoid tissue: studies on the Chorioallantoic Membrane (CAM) of the chick embryo. *J Pathol.* **1980**;132(3):191–205.
79. Su SC, Lin CW, Yang WE, et al. The Urokinase-type Plasminogen Activator (UPA) system as a biomarker and therapeutic target in human malignancies. *Expert Opin Ther Targets.* **2016**;20(5):551–566.
80. Dass K, Ahmad A, Azmi AS, et al. Evolving role of UPA/UPAR system in human cancers. *Cancer Treat Rev.* **2008**;34(2):122–136.
81. Deryugina EI, Kiosses WB. Intratumoral cancer cell intravasation can occur independent of invasion into the adjacent stroma. *Cell Rep.* **2017**;19(3):601–616.
82. Deryugina EI, Zijlstra A, Partridge JJ, et al. Unexpected effect of matrix metalloproteinase down-regulation on vascular intravasation and metastasis of human fibrosarcoma cells selected in vivo for high rates of dissemination. *Cancer Res.* **2005**;65(23):10959–10969.
83. Zuo Z, Syrovets T, Genze F, et al. MRI analysis of breast cancer xenograft on the chick chorioallantoic membrane. *NMR Biomed.* **2015**;28(4):440–447.
84. Shanmugam MK, Ahn KS, Hsu A, et al. Thymoquinone inhibits bone metastasis of breast cancer cells through abrogation of the CXCR4 signaling axis. *Front Pharmacol.* **2018**;9. DOI:10.3389/fphar.2018.01294.
85. Yousefnia S, Ghaedi K, Seyed Foroootan F, et al. Characterization of the stemness potency of mammospheres isolated from the breast cancer cell lines. *Tumor Biol.* **2019**;41:8.
86. Li Q, Cao J, He Y, et al. R5, a neutralizing antibody to robo1, suppresses breast cancer growth and metastasis by inhibiting angiogenesis via down-regulating filamin A. *Exp Cell Res.* **2020**;387(1):111756.
87. Eder S, Arndt A, Lamkowski A, et al. Baseline MAPK signaling activity confers intrinsic radioresistance to KRAS-mutant colorectal carcinoma cells by rapid upregulation of heterogeneous nuclear ribonucleoprotein K (HnRNP K). *Cancer Lett.* **2017**;385:160–167.
88. Dumartin L, Quemener C, Laklai H, et al. Netrin-1 mediates early events in pancreatic adenocarcinoma progression, acting on tumor and endothelial cells. *Gastroenterology.* **2010**;137(4):1595–1606.
89. Mesci A, Lucien F, Huang X, et al. RSPO3 is a prognostic biomarker and mediator of invasiveness in prostate cancer. *J Transl Med.* **2019**;17(1):125.
90. Hagedorn M, Javerzat S, Gilges D, et al. Accessing key steps of human tumor progression in vivo by using an avian embryo model. *Proc Natl Acad Sci U S A.* **2005**;102(5):1643–1648.
91. Swadi R, Mather G, Pizer BL, et al. Optimising the chick chorioallantoic membrane xenograft model of neuroblastoma for drug delivery. *BMC Cancer.* **2018**;18(1):28.
92. Klingenberg M, Becker J, Eberth S, et al. The chick chorioallantoic membrane as an in vivo xenograft model for burkitt lymphoma. *BMC Cancer.* **2014**;14(1):339.
93. Xiao X, Zhou X, Ming H, et al. Chick chorioallantoic membrane assay: a 3D animal model for study of human nasopharyngeal carcinoma. *PLoS One.* **2015**;10(6):1–13.
94. Schneider-Stock R, Ribatti D. The CAM assay as an alternative in vivo model for drug testing. Berlin, Heidelberg: Springer Berlin Heidelberg, **2020**:1–21. DOI:10.1007/164_2020_375.
95. Leng T, Miller JM, V; Palanker BK, et al. Chorioallantoic membrane as a model tissue for surgical retinal research and simulation. *Retina.* **2004**;24(3):427–434.
96. Jefferies B, Lenze F, Sathe A, et al. Imaging of engineered human tumors in the living chicken embryo. *Sci Rep.* **2017**;7(1):1–9.
97. Winter G, Koch ABF, Löffler J, et al. Vivo PET/MRI imaging of the chorioallantoic membrane. *Front Phys.* **2020**;8. DOI:10.3389/fphys.2020.00151.
98. Warnock G, Turtoi A, Blomme A, et al. Vivo PET/CT in a human glioblastoma chicken chorioallantoic membrane model: a new tool for oncology and radiotracer development. *J Nucl Med.* **2013**;54(10):1782–1788.
99. Winter G, Koch ABF, Löffler J, et al. PET and MR imaging in the Hen's Egg Test-Chorioallantoic Membrane (HET-CAM) model for initial in vivo testing of target-specific radioligands. *Cancers (Basel).* **2020**;12(5):5.
100. Waschkies C, Nicholls F, Buschmann J. Comparison of medetomidine, thiopental and ketamine/midazolam anesthesia in chick embryos for in ovo magnetic resonance imaging free of motion artifacts. *Sci Rep.* **2015**;5(1):15536.
101. Lin B, Song X, Yang D, et al. Anlotinib inhibits angiogenesis via suppressing the activation of VEGFR2, PDGFRbeta and FGFR1. *Gene.* **2018**;654:77–86.
102. Zhong L, Guo X-N, Zhang X-H, et al. TKI-31 inhibits angiogenesis by combined suppression signaling pathway of VEGFR2 and PDGFRbeta. *Cancer Biol Ther.* **2014**;5(3):323–330.
103. Sunitinib MC. Resistance in Renal Cell Carcinoma. *J Kidney Cancer VHL.* **2014**;1(1):1.
104. Mulet-Margalef N, Garcia-Del-Muro X. Sunitinib in the treatment of gastrointestinal stromal tumor: patient selection and perspectives. *Onco Targets Ther.* **2016**;9:7573–7582.
105. Pozas M, San Roman M, Alonso-Gordoa T, et al. Angiogenesis in pancreatic neuroendocrine tumors: resistance mechanisms. *Int J Mol Sci.* **2019**;20(19):19.
106. D'Costa NM, Lowerison MR, Raven PA, et al. Y-box binding protein-1 is crucial in acquired drug resistance development in metastatic clear-cell renal cell carcinoma. *J Exp Clin Cancer Res.* **2020**;39(1):33.
107. Cimpean AM, Lalošević D, Lalošević V, et al. Disodium cromolyn and anti-podoplanin antibodies strongly inhibit growth of BHK 21/C13-derived fibrosarcoma in a chick embryo chorioallantoic membrane model. In Vivo (Brooklyn). **2018**;32(4):791–798.
108. Ferician O, Cimpean AM, Avram S, et al. Endostatin effects on tumor cells and vascular network of human renal cell carcinoma implanted on chick embryo chorioallantoic membrane. *Anticancer Res.* **2015**;35(12):6521–6528.
109. Venkatesulu BP, Mahadevan LS, Aliru ML, et al. Vascular injury: a review of possible mechanisms. *JACC Basic Transl Sci.* **2018**;3(4):563–572.
110. Baselet B, Sonveaux P, Baatout S, et al. Pathological effects of ionizing radiation: endothelial activation and dysfunction. *Cell Mol Life Sci.* **2019**;76(4):699–728.
111. Sharma RA, Plummer R, Stock JK, et al. Clinical development of new drug-radiotherapy combinations. *Nat Rev Clin Oncol.* **2016**;13(10):627–642.
112. Dahl O, Dale JE, Brydoy M. Rationale for combination of radiation therapy and immune checkpoint blockers to improve cancer treatment. *Acta Oncol.* **2019**;58(1):9–20.
113. Yuan YJ, Xu K, Wu W, et al. Application of the chick embryo chorioallantoic membrane in neurosurgery disease. *Int J Med Sci.* **2014**;11(12):1275–1281.
114. Kähler J, Hafner S, Popp T, et al. Heterogeneous nuclear ribonucleoprotein K is overexpressed and contributes to radioresistance irrespective of HPV status in head and neck squamous cell carcinoma. *Int J Mol Med.* **2020**;46(5):1733–1742.
115. Abe C, Uto Y, Nakae T, et al. Evaluation of the in vivo radiosensitizing activity of etanidazole using tumor-bearing chick embryo. *J Radiat Res.* **2011**;52(2):208–214.
116. Dörr W. Pathogenesis of normal tissue side effects. In: Joiner MC, Van der Kogel AJ, editors. *Basic clinical radiobiology.* Taylor & Francis, Boca Raton, FL; **2018**. pp. 152–170.
117. Karnabatidis D, Dimopoulos JCA, Siablis D, et al. Quantification of the ionising radiation effect over angiogenesis in the chick embryo and its chorioallantoic membrane by computerised

- analysis of angiographic images. *Acta Radiol.* 2001;42(3):333–338.
118. Sabatasso S, Laissue JA, Hlushchuk R, et al. Tissue damage depends on the stage of vascular maturation. *Int J Radiat Oncol Biol Phys.* 2011;80(5):1522–1532.
 119. Marques FG, Poli E, Rino J, et al. Low doses of ionizing radiation enhance the angiogenic potential of adipocyte conditioned medium. *Radiat Res.* 2019;192(5):517–526.
 120. Kardamakis D, Hadjimichael C, Ginopoulos P, et al. Effects of paclitaxel in combination with ionizing radiation on angiogenesis in the chick embryo chorioallantoic membrane. a radiobiological study. *Strahlenther Onkol.* 2004;180(3):152–156.
 121. Mahvi DA, Liu R, Grinstaff MW, et al. Local cancer recurrence: the realities, challenges, and opportunities for new therapies. *CA Cancer J Clin.* 2018;68(6):488–505.
 122. Bobo D, Robinson KJ, Islam J, et al. Nanoparticle-based medicines: a review of FDA-approved materials and clinical trials to date. *Pharm Res.* 2016;33(10):2373–2387.
 123. Cassano D, Pocić-Martínez S, Ultrasmall-in-Nano Approach VV. Enabling the translation of metal nanomaterials to clinics. *Bioconjug Chem.* 2018;29(1):4–16.
 124. Blanco E, Shen H, Ferrari M. Principles of nanoparticle design for overcoming biological barriers to drug delivery. *Nat Biotechnol.* 2015;33(9):941–951.
 125. Bouchoucha M, Côté MF, Gaudreault C, et al. Mesoporous silica nanoparticles for tunable drug release and enhanced anti-tumoral activity. *Chem Mater.* 2016;28(12):4243–4258.
 126. Yildiz I, Shukla S, Steinmetz NF. Applications of viral nanoparticles in medicine. *Curr Opin Biotechnol.* 2011;22(6):901–908.
 127. Shukla S, Ablack AL, Wen AM, et al. Increased tumor homing and tissue penetration of the filamentous plant viral nanoparticle potato virus X. *Mol Pharm.* 2013;10(1):33–42.
 128. Cho CF, Ablack A, Leong HS, et al. Evaluation of nanoparticle uptake in tumors in real time using intravital imaging. *J Vis Exp.* 2011;No. 52:7–11. DOI:10.3791/2808.
 129. Suk JS, Xu Q, Kim N, et al. PEGylation as a strategy for improving nanoparticle-based drug and gene delivery. *Adv Drug Deliv Rev.* 2016;99:28–51.
 130. Tenzer S, Docter D, Kuharev J, et al. Rapid formation of plasma protein corona critically affects nanoparticle pathophysiology. *Nat Nanotechnol.* 2013;8(10):772–781.
 131. Lunov O, Syrovets T, Loos C, et al. Differential uptake of functionalized polystyrene nanoparticles by human macrophages and a monocytic cell line. *ACS Nano.* 2011;5(3):1657–1669.
 - **This study illustrates the preferential binding of NPs to tumor cells than avian cells using a specific chicken macrophage marker (KUL01).**
 132. Loos C, Syrovets T, Musyanovych A, et al. Nanoparticles as Inhibitors of MTOR and inducers of cell cycle arrest in leukemia cells. *Biomaterials.* 2014;35(6):1944–1953.
 133. Medinger M, Passweg J. Angiogenesis in myeloproliferative neoplasms, new markers and future directions *Memo - Mag. Eur Med Oncol.* 2014;7(4):206–210.
 134. Han Y, Wang X, Wang B, et al. The Progress of Angiogenic Factors in the Development of Leukemias. *Intractable Rare Dis Res.* 2016;5(1):6–16.
 135. Bazak R, Houry M, El Achy S, et al. Cancer active targeting by nanoparticles: a comprehensive review of literature. *J Cancer Res Clin Oncol.* 2015;141(5):769–784.
 136. Chen Y, Tezcan O, Li D, et al. Overcoming multidrug resistance using folate receptor-targeted and PH-responsive polymeric nanogels containing covalently entrapped doxorubicin. *Nanoscale.* 2017;9(29):10404–10419.
 137. Steinmetz NF, Ablack AL, Hickey JL, et al. Intravital imaging of human prostate cancer using viral nanoparticles targeted to gastrin-releasing peptide receptors. *Small.* 2011; 7 ;12, 1664–1672.
 138. Niemelä E, Desai D, Niemi R, et al. Nanoparticles carrying fingolimod and methotrexate enables targeted induction of apoptosis and immobilization of invasive thyroid cancer. *Eur J Pharm Biopharm.* Dec 2019;2020(148):1–9.
 139. Rogosnitzky M, Branch S. Gadolinium-based contrast agent toxicity: a review of known and proposed mechanisms. *BioMetals.* 2016;29(3):365–376.
 140. Zuo Z, Syrovets T, Wu Y, et al. The CAM cancer xenograft as a model for initial evaluation of MR labelled compounds. *Sci Rep.* 2017;7(1):46690.
 141. Faucher L, Guay-Bégin AA, Lagueux J, et al. Ultra-small gadolinium oxide nanoparticles to image brain cancer cells in vivo with MRI. *Contrast Media Mol Imaging.* 2011;6(4):209–218.
 142. Corem-Salkmon E, Perlstein B, Margel S. Design of near-infrared fluorescent bioactive conjugated functional iron oxide nanoparticles for optical detection of colon cancer. *Int J Nanomedicine.* 2012;7:5517–5527.
 143. Jendželovská Z, Jendželovský R, Kuchárová B, et al. Hypericin in the light and in the dark: two sides of the same coin. *Front Plant Sci.* 2016;7:1–20.
 144. Zeisser-Labouèbe M, Delie F, Gurny D, et al. Screening of nanoparticulate delivery systems for the photodetection of cancer in a simple and cost-effective model. *Nanomedicine.* 2009;4(2):135–143.
 145. Voliani V, González-Béjar M, Herranz-Pérez V, et al. Orthogonal functionalisation of upconverting NaYF₄ nanocrystals. *Chem Eur J.* 2013;19(40):13538–13546.
 146. Wang M, Abbineni G, Clevenger A, et al. Upconversion nanoparticles: synthesis, surface modification and biological applications. *Nanomed Nanotechnol Biol Med.* 2011;7(6):710–729.
 147. Grodzik M, Sawosz E, Wierzbicki M, et al. Nanoparticles of carbon allotropes inhibit glioblastoma multiforme angiogenesis in ovo. *Int J Nanomedicine.* 2011;6:3041.
 148. Urbańska K, Pająk B, Orzechowski A, et al. The effect of silver nanoparticles (AgNPs) on proliferation and apoptosis of in ovo cultured Glioblastoma Multiforme (GBM) cells. *Nanoscale Res Lett.* 2015;10(1):1.
 149. Kutwin M, Sawosz E, Jaworski S, et al. Investigation of platinum nanoparticle properties against U87 glioblastoma multiforme. *Arch Med Sci.* 2017;13(6):1322–1334.
 150. Liu LZ, Ding M, Zheng JZ, et al. Tungsten carbide-cobalt nanoparticles induce reactive oxygen species, AKT, ERK, AP-1, NF-κB, VEGF, and Angiogenesis. *Biol Trace Elem Res.* 2015;166(1):57–65.
 151. Vargas A, Pegaz B, Debeve E, et al. Improved photodynamic activity of porphyrin loaded into nanoparticles: an in vivo evaluation using chick embryos. *Int J Pharm.* 2004;286(1–2):131–145.
 152. Cassano D, Santi M, Cappello V, et al. Biodegradable passion fruit-like nano-architectures as carriers for cisplatin prodrug *part.* *Part Syst Charact.* 2016;33(11):818–824.
 153. Mapanao AK, Santi M, Faraci P, et al. Endogenously-triggerable ultrasmall-in-nano architectures: targeting assessment on 3D pancreatic carcinoma spheroids. *ACS Omega.* 2018;3(9):11796–11801.
 154. Bikhezar F, de Kruijff RM, van der Meer AJGM, et al. Preclinical evaluation of binimetinib (MEK162) delivered via polymeric nanocarriers in combination with radiation and temozolomide in glioma. *J Neurooncol.* 2020;146(2):239–246.
 155. Barenholz Y. (Chezy). Doxil® — the first FDA-approved nano-drug: lessons learned. *J Control Release.* 2012;160(2):117–134.
 156. Vu BT, Shahin SA, Croissant J, et al. Chick chorioallantoic membrane assay as an in vivo model to study the effect of nanoparticle-based anticancer drugs in ovarian cancer. *Sci Rep.* 2018;8(1):8524.
 - **The authors demonstrate the advantageous selective tumor accumulation of nano-encapsulated doxorubicin compared to the administered free drug solution that was also found in off-site (harvested) organs.**
 157. Yalcin M, Bharali DJ, Lansing L, Dyskin E, Mousa SS, Herbergs A, Davis FB, Davis PJ, Mousa SA. Tetraiodothyroacetic acid (Tetrac) and tetrac nanoparticles inhibit growth of human renal cell carcinoma xenografts. *Anticancer Res.* 2009;29(10):3825–3831.

158. Paris JL, Villaverde G, Gómez-Graña S, et al. Nanoparticles for multimodal antivasular therapeutics: dual drug release, photothermal and photodynamic therapy. *Acta Biomater.* 2020;101:459–468.
159. Elsadek B, Kratz F. Impact of albumin on drug delivery - new applications on the horizon. *J Control Release.* 2012;157(1):4–28.
160. Hafner S, Raabe M, Wu Y, et al. Resonance imaging and efficient delivery of an albumin nanotheranostic in triple-Negative breast cancer xenografts. *Adv Ther.* 2019;2(11):1900084.
161. Garrier J, Reshetov V, Gräfe S, et al. Factors affecting the selectivity of nanoparticle-based photoinduced damage in free and xenografted chorioallantoic membrane model. *J Drug Target.* 2014;22(3):220–231.
162. Riley II M, Vermerris W. Recent advances in nanomaterials for gene delivery—A review. *Nanomaterials.* 2017;7(5):94.
163. Masjedi A, Ahmadi A, Atyabi F, et al. Silencing of IL-6 and STAT3 by siRNA loaded hyaluronate-N,N,N-trimethyl chitosan nanoparticles potentially reduces cancer cell progression. *Int J Biol Macromol.* 2020;149:487–500.
164. Kilarski WW, Samolov B, Petersson L, et al. Biomechanical regulation of blood vessel growth during tissue vascularization. *Nat Med.* 2009;15(6):657–664.
165. Zudaire E, Gambardella L, Kurcz C, et al. Tool for quantitative analysis of vascular networks. *PLoS One.* 2011;6(11):1–12.
166. Ribatti D, Nico B, Perra MT, et al. Erythropoietin is involved in angiogenesis in human primary melanoma. *Int J Exp Pathol.* 2010;91(6):495–499.
167. Beckers M, Gladis-Villanueva M, Hamann W, et al. Use of the chorio-allantoic membrane of the chick embryo as test for anti-inflammatory activity. *Inflamm Res.* 1997;46(1):29–30.
168. Stephens DJ, Allan VJ. Light microscopy techniques for live cell imaging. *80 Science.* 2003;300(5616):82–86.
169. Pink DBS, Schulte W, Parseghian MH, et al. Quantitation of vascular permeability in vivo: implications for drug delivery. *PLoS One.* 2012;7(3):1–10.
170. Jilani SM, Murphy TJ, Thai SNM, et al. Selective binding of lectins to embryonic chicken vasculature. *J Histochem Cytochem.* 2003;51(5):597–604.
171. Vargas A, Eid M, Fanchaouy M, et al. In vivo photodynamic activity of photosensitizer-loaded nanoparticles: formulation properties, administration parameters and biological issues involved in PDT outcome. *Eur J Pharm Biopharm.* 2008;69(1):43–53.
172. Mamaeva V, Niemi R, Beck M, et al. Inhibiting notch activity in breast cancer stem cells by glucose functionalized nanoparticles carrying γ -secretase inhibitors. *Mol Ther.* 2016;24(5):926–936.
173. Nowak-Sliwinska P, Alitalo K, Allen E, et al., Consensus guidelines for the use and interpretation of angiogenesis assays, *Angiogenesis* 2018:Vol. 21, DOI:10.1007/s10456-018-9613-x.
174. Leong HS, Steinmetz NF, Ablack A, et al. Intravital imaging of embryonic and tumor neovasculature using viral nanoparticles. *Nat Protoc.* 2010;5(8):1406–1417.
175. Jonkman J, Brown CM. Any way you slice it—A comparison of confocal microscopy techniques. *J Biomol Tech.* 2015;26(2):54–65.
176. MacDonald IC, Schmidt EE, Morris VL, et al. Intravital videomicroscopy of the chorioallantoic microcirculation: a model system for studying metastasis. *Microvasc Res.* 1992;44(2):185–199.
177. Wilcox JN. Fundamental principles of in situ hybridization. *J Histochem Cytochem.* 1993;41(12):1725–1733.
178. Javerzat S, Franco M, Herbert J, et al. Correlating global gene regulation to angiogenesis in the developing chick extra-embryonic vascular system. *PLoS One.* 2009;4(11):11.
179. Deininger PL, Batzer MA. Alu repeats and human disease. *Mol Genet Metab.* 1999;67(3):183–193.
180. Wierzbicki M, Sawosz E, Grodzik M, et al. Comparison of anti-angiogenic properties of pristine carbon nanoparticles. *Nanoscale Res Lett.* 2013;8(1):1–8.
181. Deryugina EI, Bourdon MA, Reisfeld RA, et al. Remodeling of collagen matrix by human tumor cells requires activation and cell surface association of matrix metalloproteinase-2. *Cancer Res.* 1998;58(16):3743–3750.
182. Büchele B, Zugmaier W, Genze F, et al. High-performance liquid chromatographic determination of acetyl-11-Keto- α -boswellic acid, a novel pentacyclic triterpenoid, in plasma using a fluorinated stationary phase and photodiode array detection: application in pharmacokinetic studies. *J Chromatogr B Anal Technol Biomed Life Sci.* 2005;829(1–2):144–148.
183. Honda N, Kariyama Y, Hazama H, et al. Optical properties of tumor tissues grown on the chorioallantoic membrane of chicken eggs: tumor model to assay of tumor response to photodynamic therapy. *J Biomed Opt.* 2015;20(12):125001.
184. Fotinos N, Campo MA, Popowycz F, et al. 5-aminolevulinic acid derivatives in photomedicine: characteristics, application and perspectives. *Photochem Photobiol.* 2006;82(4):994.
185. DuFort CC, DelGiorno KE, Hingorani SR. Mounting pressure in the microenvironment: fluids, solids, and cells in pancreatic ductal adenocarcinoma. *Gastroenterology.* 2016;150(7):1545–1557 e2.
186. Schnittert J, Bansal R, Prakash J. Targeting pancreatic stellate cells in cancer. *Trends Cancer.* 2019;5(2):128–142.
187. Soulet F, Kilarski WW, Roux-Dalvai F, et al. Mapping the extracellular and membrane proteome associated with the vasculature and the stroma in the embryo. *Mol Cell Proteomics.* 2013;12(8):2293–2312.
- **First description of the vascular and matrix proteome of the chick embryo and comparisons made against wound and glioblastoma-grafted CAM.**
188. Giannopoulou E, Katsoris P, Hatzia Apostolou M, et al. Extracellular matrix in vivo. *Int J Cancer.* 2001;94(5):690–698.
189. Papadimitriou E, Unsworth BR, Maragoudakis ME, et al. Quantification of extracellular matrix maturation in the chick chorioallantoic membrane and in cultured endothelial cells. *Endothelium.* 1993;1(3):207–219.
- **This study shows the quantification CAM-derived ECM proteins in a time-course dependent manner.**
190. Sahai E, Astsaturov I, Cukierman E, et al. A framework for advancing our understanding of cancer-associated fibroblasts. *Nat Rev Cancer.* 2020;20(3):174–186.
191. Schneiderhan W, Diaz F, Fundel M, et al. Pancreatic stellate cells are an important source of MMP-2 in human pancreatic cancer and accelerate tumor progression in a murine xenograft model and CAM assay. *J Cell Sci.* 2007;120(Pt 3):512–519.
192. Chojnacka-Puchta L, Sawicka D CRISPR/Cas9 gene editing in a chicken model: current approaches and applications. *Journal of Applied Genetics.* 2020;61:221–229. DOI:10.1007/s13353-020-00537-9.
193. Sid H, Schusser B Applications of gene editing in chickens: a new era is on the horizon. *Frontiers in Genetics.* 2018;9:456. DOI:10.3389/fgene.2018.00456.